AJS American Journal of Science
publishing earth-sciences research since 1818

Lowe, D. R., & Byerly, G. R. (2024). Geology of the Eastern Barberton Greenstone Belt, South Africa: Early Deformation and the Role of Large Meteor Impacts. *American Journal of Science*, *324*, 12. https://doi.org/10.2475/001c.122938

Science Paper

Geology of the Eastern Barberton Greenstone Belt, South Africa: Early Deformation and the Role of Large Meteor Impacts

Donald R. Lowe[1][a], Gary R. Byerly[2]

[1] Department of Earth and Planetary Sciences, Stanford University, [2] Department of Geology and Geophysics, Louisiana State University

Keywords: Archean, Barberton Greenstone Belt, Fig Tree Group, Archean impacts, Archean sedimentation, Archean tectonics

https://doi.org/10.2475/001c.122938

American Journal of Science

Vol. 324, 2024

The eastern Barberton Greenstone Belt (BGB) includes four stratigraphic and structural divisions: from northwest to southeast, the Mlumati, Manzimnyama, and Paulus Synclines and the Emlembe Belt. All are made up largely of sedimentary rocks of the Fig Tree Group separated by antiformal belts of sheared Onverwacht Group komatiitic rocks. Fig Tree rocks in the Mlumati and Manzimnyama Synclines are mostly chemically precipitated banded iron formation (BIF) and banded ferruginous chert (BFC) with a major siliciclastic unit, the Gelegela Grit, composed of quartz-poor (<5% monocrystalline quartz, Qm) volcaniclastic sandstone showing abundant ~3.445–3.455 Ga detrital zircons. The Paulus Syncline is dominated by shale containing in the upper half chert-clast conglomerate and sparse lithic sandstone (Qm<10%) but includes near the middle lenticular units up to unit 30 m thick of quartz-rich (Qm >50%) sandstone. The Emlembe Belt consists largely of chert-clast conglomerate and quartz-bearing (Qm = 10–50%) sandstone. The Paulus and Emlembe belts show detrital zircon age peaks at ~3.295–3.275 Ga and ~3.445–3.455 Ga. While exhibiting overall similar stratigraphic development and detrital zircon ages, Fig Tree rocks in these belts show contrasting compositions and sediment sources. They do not represent parts a single basin or fairway of sediment transport and deposition.

Fig Tree siliciclastic rocks mark the first deformation, uplift, and erosion in the BGB. However, the thinness of Fig Tree strata, mostly less than 1000 m, and rapid facies changes argue that deformation involved local uplifts and small basins that accumulated thin sedimentary sequences. We suggest that early Fig Tree deformation is consistent with crustal disruption triggered by large meteor impacts, starting perhaps as early as ~3.277 Ga but certainly by ~3.260 Ga. The Fig Tree Group may record a cluster of impacts that fragmented and destabilized a long-lived crust followed during later or post-Fig Tree time by tectonic uplift and orogeny.

1. INTRODUCTION

The 3.55 to 3.22 Ga Barberton Greenstone Belt (BGB) in southern Africa has provided a wealth of detail about the nature and evolution of the early crust, its life, atmosphere, oceans, and surface environments. The BGB is made up of deformed, mostly low-grade metasedimentary and metavolcanic rocks of the Barberton Supergroup that have been divided into three main stratigraphic units (figs. 1 & 2): from base to top the Onverwacht, Fig Tree, and Moodies Groups (Byerly et al., 2018; Lowe & Byerly, 1999; M. J. Viljoen & Viljoen, 1969; R. P. Viljoen & Viljoen, 1969). The 10–12 km thickness of the Onverwacht Group represents nearly 300 myr dominated by anorogenic komatiitic to basaltic volcanism terminated by uplift and deformation represented by siliciclastic sedimentary rocks of the Fig Tree and Moodies Groups. In the present discussion, we will focus on sedimentary rocks of the 3.277–3.225-Ga Fig Tree Group in the eastern part of the BGB, their stratigraphic and sedimentological development, and what these and similar units throughout the BGB tell us about one of the Earth's earliest periods of uplift, deformation, and siliciclastic sedimentation.

Lowe et al. (1999) divided the southern BGB in South Africa (fig. 1A) into four stratigraphic and structural blocks termed from NW to SE the Northern (ND), West-Central (WCD), East-Central (ECD), and Southern (SD) Domains (fig. 1B). Heinrichs (1980) mapped parts of what we term the ECD and defined a series of new formations and members within the Fig Tree Group that have been incorporated

a Corresponding author: drlowe@stanford.edu

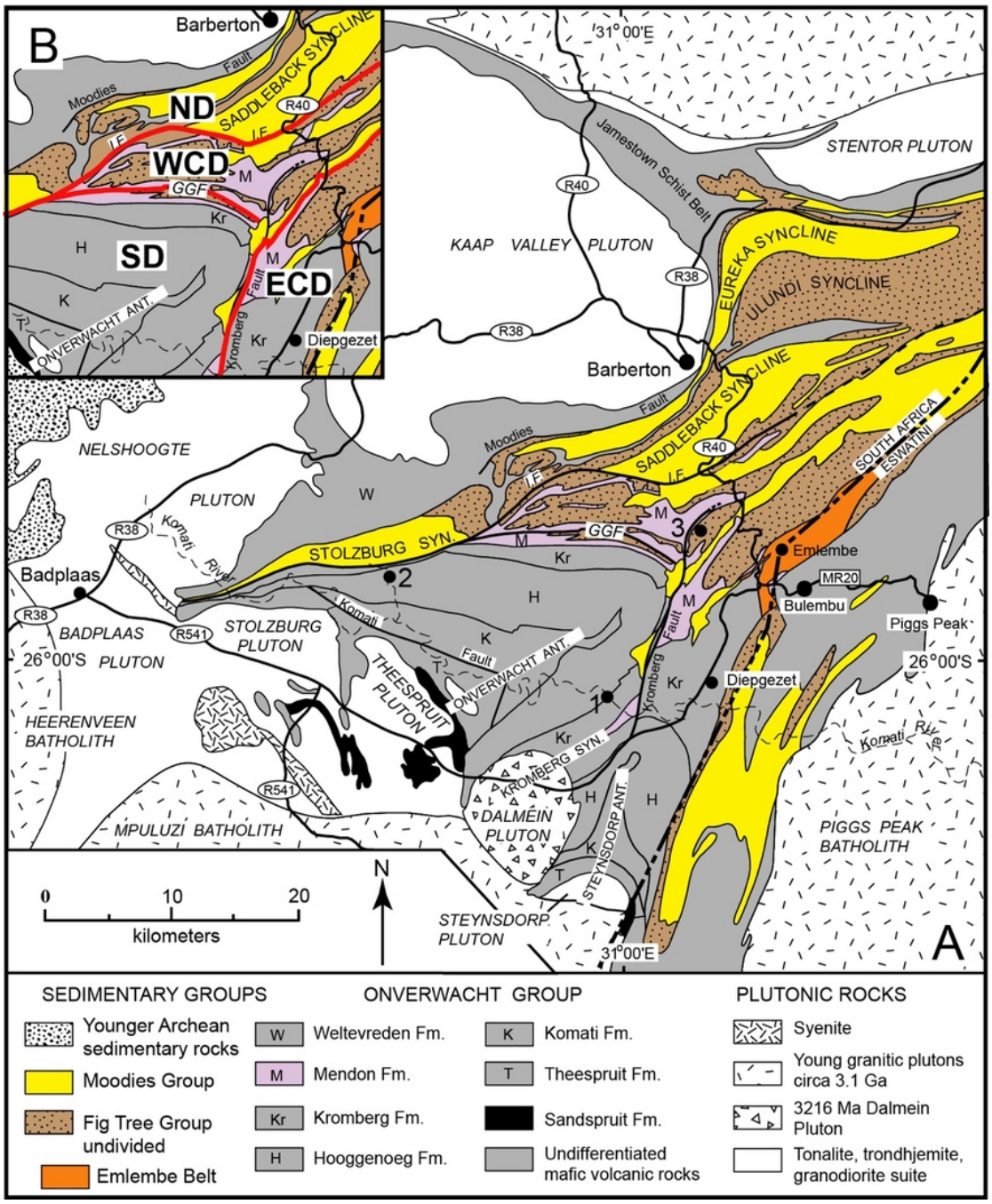

Figure 1. General geology of the Barberton Greenstone Belt. (A) Geologic map and stratigraphic units of the southwestern part of the BGB. Symbols: I.F., Inyoka Fault; GGF, Granville Grove Fault. Localities mentioned in text: 1, Komati Gorge section of the upper Hooggenoeg and Kromberg Formations; 2, Mawelawela River section of the upper Hooggenoeg Formation; 3, Barite Valley area. (B) Inset showing the location of the four domains in the western Barberton Belt: ND, Northern Domain; WCD, West-Central Domain (north of Granville Grove and south of Inyoka Faults); SD, Southern Domain (south of Granville Grove Fault); ECD, East-Central Domain.

into recent discussions of ECD geology (Drabon, Galić, et al., 2019; Stoll et al., 2021). Lamb (1984), Lamb and Paris (1988), and Paris (1984) mapped and reported on parts of the ECD mostly south of the present study area. Investigations of Drabon and Lowe (2022), Harrington (2017), Heubeck (1993), Heubeck and Lowe (1999), Lowe et al. (2012), Stoll (2020), Stoll et al. (2021), and Zentner (2014) have outlined the basic distribution, stratigraphy, sedimentology, and ages of ECD rocks.

These studies have revealed three key aspects of ECD geology: (1) Lamb (1984) and Lamb and Paris (1988) emphasized that the classic Fig Tree-Moodies lithologic contrasts seen in the northern parts of the BGB, where Fig Tree sandstones are quartz and feldspar poor and overlying Moodies sandstones are quartz and feldspar rich, break down in eastern and southeastern parts of the belt where quartz-rich rocks are apparently more common in units that might otherwise be considered to be Fig Tree in age and strati-

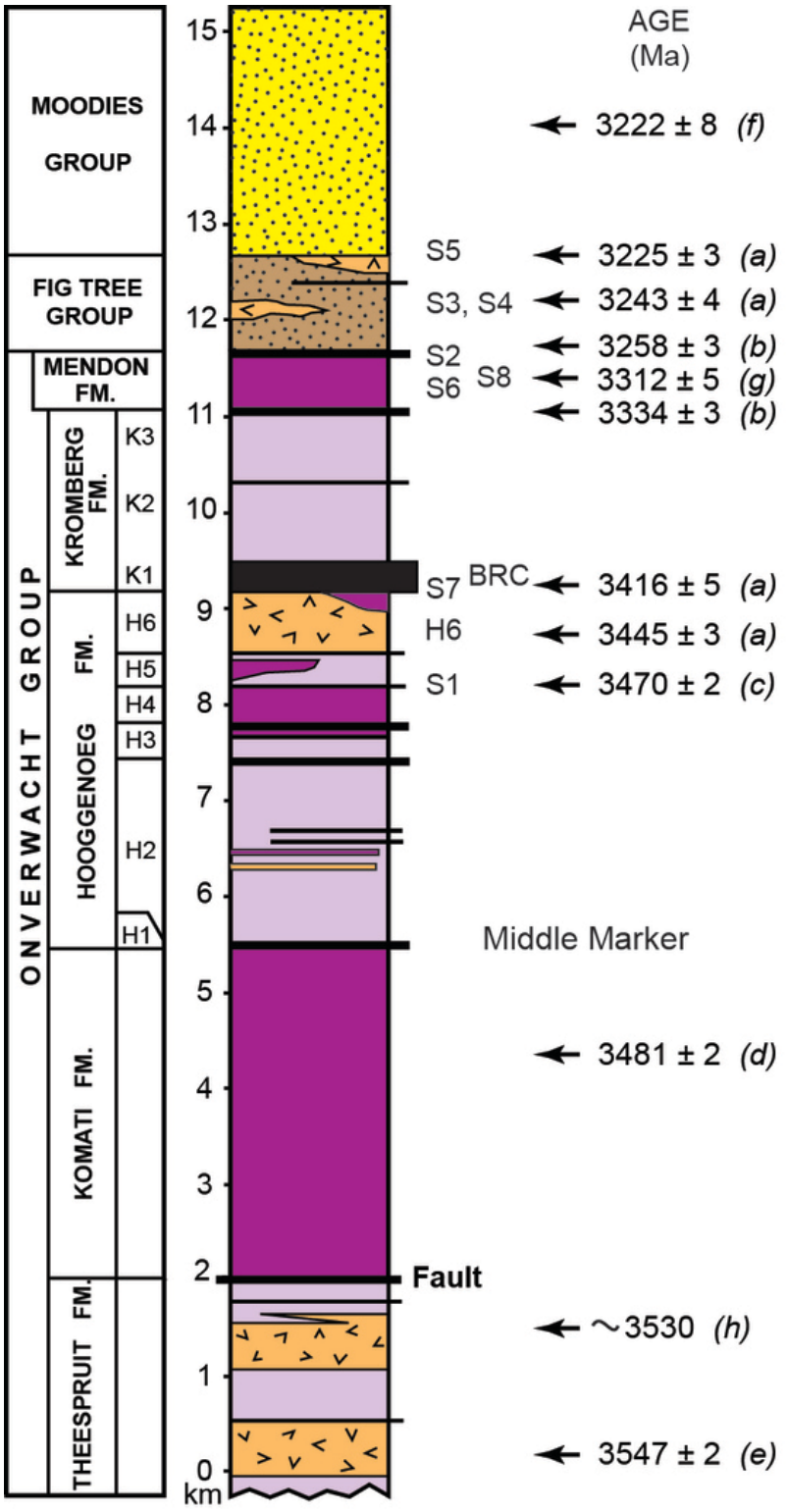

Figure 2. General stratigraphic column of rocks of the Barberton Greenstone Belt, South Africa, showing key ages in myr and stratigraphic positions of the Buck Reef Chert (BRC) and the known impact layers, S1 through S8. All ages are U-Pb ages on zircons. References for ages and for precise dating methodology are below (a through h). Key: cherty sedimentary units (black), komatiitic volcanic rocks (purple), basaltic volcanic rocks (mauve), felsic volcanic rocks (orange), Fig Tree Group siliciclastic rocks (brown), and Moodies Group siliciclastic rocks (yellow). References for ages: (a) Kröner et al. (1991); (b) Byerly et al. (1996); (c) Byerly et al. (2002); (d) Dann (2000); (e) Kröner et al. (1996); (f) Heubeck et al. (2013); (g) Drabon et al. (2017); (h) Van Kranendonk et al. (2009).

graphic position and where feldspar is largely lacking in rocks considered to be part of the Moodies Group. (2) In the WCD the base of the Fig Tree Group is marked by a distinctive bed containing spherical particles, termed spherules, interpreted to have formed by the condensation of a rock vapor cloud produced by a large meteor impact (Lowe et al., 2003; Lowe & Byerly, 1986, 2018). This layer has been termed spherule bed S2 and dated at 3.258±3 Ga (Byerly et al., 1996). In the ND the base of the Fig Tree Group is also marked by an impact layer, spherule bed S3, dated at 3.243±4 Ga (Kröner et al., 1991). Neither S2 nor S3 has been identified in the ECD and confirmed ages of Fig Tree rocks in the ECD range from ~3.277 Ga at the base to ~3.260 Ga in the upper part (Drabon et al., 2017; Drabon & Lowe, 2022; Stoll et al., 2021). The apparent absence of marker spherule beds in the ECD, the substantially older base of the Fig Tree Group, and the absence of detrital zircon age peaks younger than ~3.260 Ga (Drabon et al., 2017; Drabon & Lowe, 2022; Stoll et al., 2021) suggest that most or all Fig Tree rocks preserved in the ECD may be older than Fig Tree rocks in the WCD and ND.

(3) From the Mlumati and Manzimnyama Synclines southeast to the Paulus Syncline and Emlembe Belt (figs. 3 & 4), post-Onverwacht rocks show a regular increase in the abundance of conglomerate and coarse sandstone, a decrease in the proportions of banded iron formation and banded ferruginous chert, and the transition from deep- to shallow-water or even terrestrial sedimentation. These trends could reflect transitions from distal, deep-water to proximal, shallow water or terrestrial settings within a large Fig Tree basin (Drabon & Lowe, 2022; Lowe, 1999a). Drabon and Lowe (2022) have suggested that the younging of the age of inception of Fig Tree sedimentation across the BGB from SE to NW reflects the progradation of a northwest-verging fold and thrust belt and the migration of the locus of foreland basin sedimentation toward the northwest. Stoll et al. (2021) argued that the geochemistry and petrology of siliciclastic sediments across the belts indicate different source rocks for the sediments in each belt, suggesting that the ECD sequence does not represent a single major shallow- to deep-water transport and depositional fairway. In many respects, however, the idea of a single large integrated Fig Tree basin in the ECD versus multiple basins or disparate parts of a large, complex basin remains untested.

Because of the contrasting ages of the inception of Fig Tree sedimentation in areas southeast of The Heights Syncline, where Fig Tree deposition started at about ~3.277 Ga, and in areas to the NW of The Heights Syncline, where Fig Tree deposition started at ~3.258 Ga or younger, we have redefined the ECD in this study to include only areas southeast of The Heights Syncline (fig. 1B) where there is an older age (~3.277 Ga) of initial Fig Tree sedimentation. Areas previously assigned to the ECD but NW of The Heights Syncline, including the Barite Valley area, where the ~3.258 Ga S2 impact layer marks the base of the Fig Tree Group, are here included in the WCD (fig. 1B).

The present study draws on published as well as new data and mapping by the authors and their students over the past 15 years. It has two main objectives: (1) to increment and synthesize data on the stratigraphy, structure, and provenance of post-Onverwacht rocks in the ECD, and (2) to use this information combined with details of Fig Tree stratigraphy and sedimentology from throughout the BGB to offer an alternative interpretation of early Fig Tree deformation.

2. GEOLOGIC SETTING

2.1. General Geology

The classic Onverwacht Group in the Southern Domain (figs. 1 & 2) includes 10–12 km of exposed volcanic and sedimentary rocks ranging in age from ~3.547 Ga (Kröner et al., 1996) to ~3.258 Ga (Kröner et al., 1991) that are grouped into 5 formations (fig. 2): from base to top the Theespruit, Komati, Hooggenoeg, Kromberg, and Mendon Formations. These consist largely of thick units of komatiitic and basaltic volcanic rock and at least two major felsic volcanic units (fig. 2): felsic schists and felsic breccias >3.50 Ga in the Theespruit Formation (M. J. Viljoen & Viljoen, 1969) and up to 1 km of felsic volcaniclastic strata and shallow, hypabyssal intrusions ~3.47–3.43 Ga in member H6 of the Hooggenoeg Formation (Lowe & Byerly, 1999, 2020; R. P. Viljoen & Viljoen, 1969). Mostly thin units of silicified sediments, now largely cherts, mark intervals of local volcanic quiescence (Lowe, 1999b) (fig. 2).

South of the Inyoka Fault (fig. 1) the uppermost part of the Onverwacht Group is a cyclic unit, the Mendon Formation, that ranges from ~300 m to over 1000 m thick and from ~3.334±0.003 Ga to ~3.258±0.003 Ga (Byerly, 1999; Byerly et al., 1996). The Mendon Formation is composed of alternating units of komatiitic volcanic rock, 50 to over 300 m thick, and thinner intervening silicified sedimentary layers from <5 to about 30 m thick. The uppermost layer is a regional unit of black and banded chert up to 100 m thick marking what may have been a prolonged interval of volcanic quiescence before the start of Fig Tree siliciclastic sedimentation. North of the Inyoka Fault, the Weltevreden Formation forms the Onverwacht Group. It is composed largely of komatiitic flow rocks, komatiitic tuffs, layered ultramafic igneous bodies, and sparse thin cherts representing silicified sediments (Anhaeusser, 2001; Huber & Byerly, 2018; Lowe & Byerly, 1999; Stiegler et al., 2012). The Weltevreden Formation pre-dates impact layer S3 at ~3.243 Ga, which marks the base of the Fig Tree Group in the ND and directly overlies Weltevreden komatiites and cherts.

Rocks of the overlying Fig Tree Group were deposited mainly as terrigenous siliciclastic sediments but the stratigraphy and depositional settings are highly variable across the BGB with lenticular conglomerates and lithic sandstones occurring at many levels interspersed with shale, ferruginous cherts and iron formation, and volcaniclastic units (e.g., Condie et al., 1970; Lowe & Byerly, 1999; Lowe & Nocita, 1999). In the Northern Domain, the Fig Tree Group includes the formations of Condie et al. (1970): a thin cherty Ulundi Formation at the base, a 500± m-thick unit of lithic sandstone named the Sheba Formation, and an upper unit, the Belvue Road Formation of felsic ash,

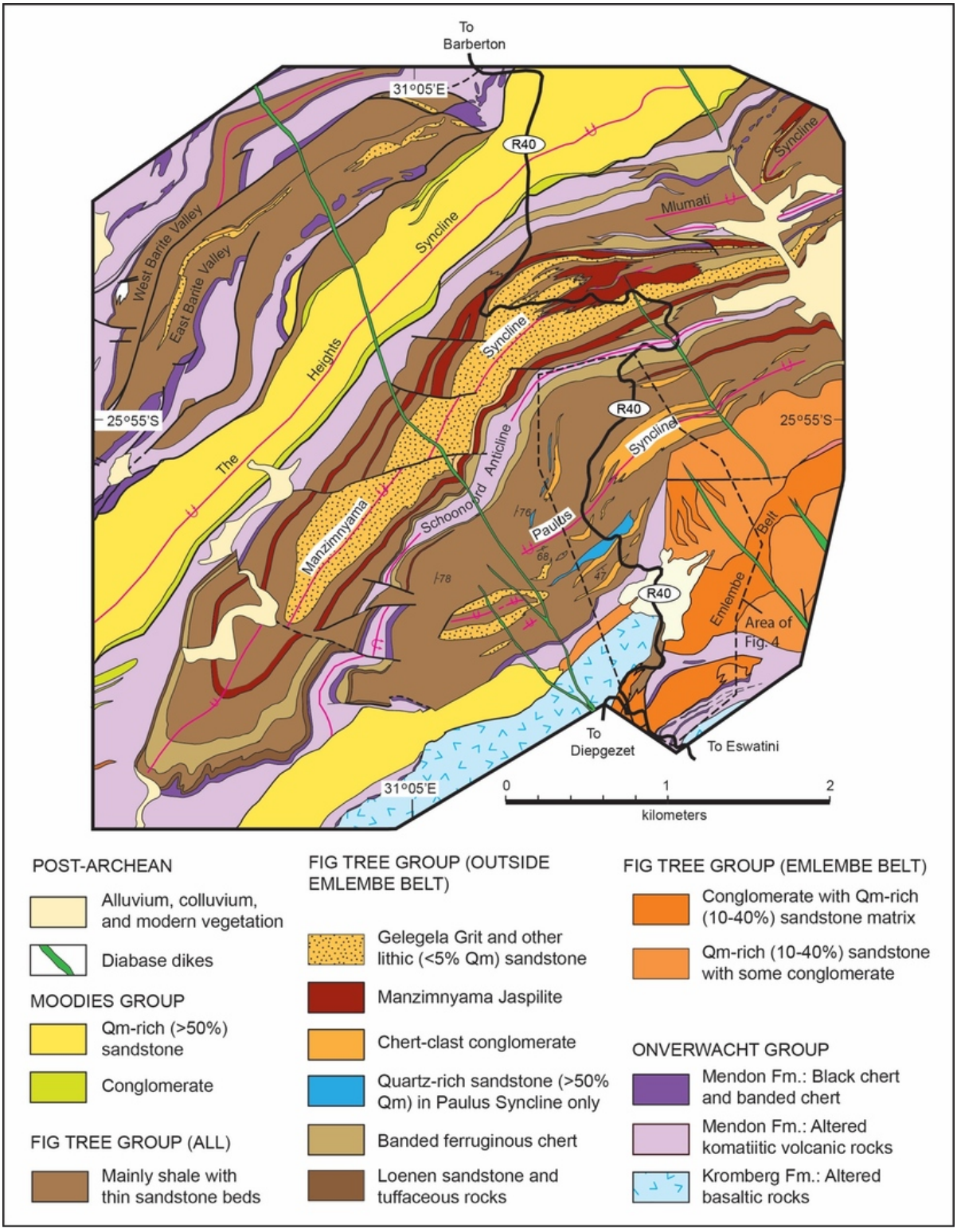

Figure 3. Geology of the ECD southeast of The Heights Syncline and the adjacent part of the WCD northwest of The Heights Syncline. The main ECD structural belts include the Mlumati, Manzimnyama, and Paulus Synclines and the more complex Emlembe Belt. All of the ECD belts appear to lack impact-related spherule beds. The lower Fig Tree Group in the WCD northwest of The Heights Syncline includes spherule beds S2 and S3 in both the East and West Barite Valley areas (Lowe et al., 2019).

mudstone, and shale. In the WCD, Fig Tree strata have been assigned to the Mapepe Formation (Lowe & Byerly, 1999). In the ECD, formations and members defined by Heinrichs (1980) can be identified in the Manzimnyama Syncline but are less easily distinguished farther to the southeast.

Rocks of the Moodies Group occur within separate structural belts, also mainly synclines or dismembered syn-

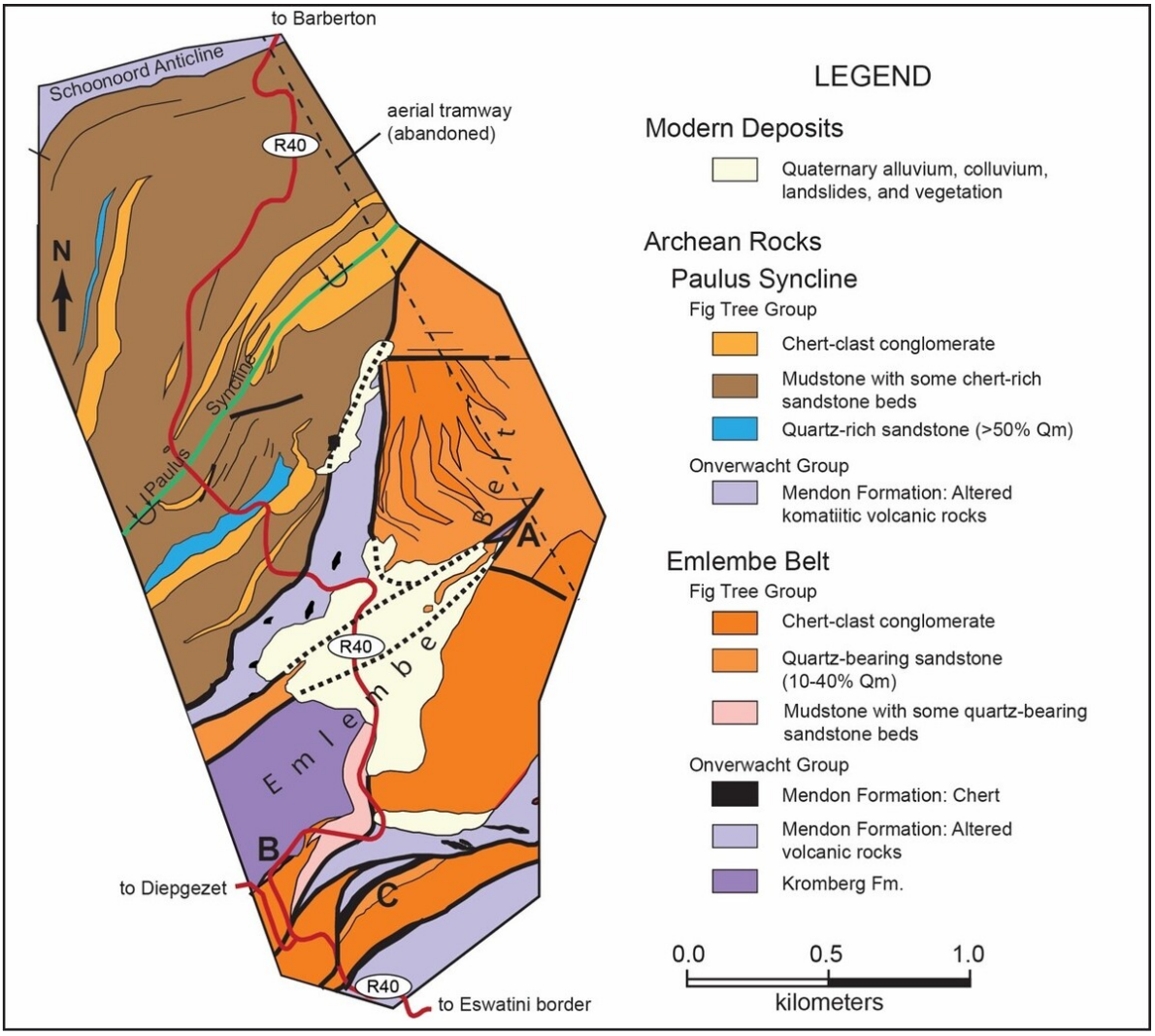

Figure 4. Geology of the eastern part of the ECD showing the Paulus Syncline and the Emlembe Belt. A, B, and C refer to localities discussed in the text. The eastern and western branches of the Emlembe Belt are separated west of R40 by a belt of Kromberg Formation volcanic rocks. The branches merge to the north at A, where the northernmost Kromberg rocks were seen.

clines, in which quartzose Moodies strata are underlain by relatively thin discontinuous units of Fig Tree felsic volcanic and volcaniclastic rocks that appear to rest conformably on altered cherts and komatiites of the Onverwacht Group (Lowe & Byerly, 1999). These felsic units include the Schoongezicht Formation in the ND (Condie et al., 1970) and Auber Villiers Formation in the WCD (Lowe & Byerly, 1999). Nowhere have we seen the thicker, predominantly siliciclastic formations of the Fig Tree Group, such as the formations of Condie et al. (1970), the Mapepe Formation of Lowe and Byerly (1999), or the units of Heinrichs (1980) in the ECD, overlain in stratigraphic sequence by felsic volcanic rocks and/or by rocks of the Moodies Group. Everywhere there appears to be a significant fault separating these sequences (Byerly et al., 2018; Lowe et al., 1999).

Rocks in the BGB are heavily deformed, generally with dips exceeding 60° and most are subvertical to overtured. Tight, often steeply plunging folds and large- to small-scale faulting are pervasive (Lowe et al., 2012; M. J. Viljoen & Viljoen, 1969; R. P. Viljoen & Viljoen, 1969). Much of the BGB can be described in terms of synclines or partial synclines made up of Fig Tree or Moodies rocks separated by narrow, often faulted anticlines composed of sheared Onverwacht rocks. Major exceptions to this type of structural style are the large, vertically plunging to overturned folds, the Onverwacht Anticline, Kromberg Syncline, and Steynsdorp Anticline, that make up the Southern Domain (fig. 1). Over large areas, including those discussed here, strain has been partitioned into more ductile units and most cherts, sandstones, and many volcanic units, are relatively free of penetrative shear fabrics.

2.2. Sandstone Composition and Alteration

Rocks in the BGB have widely seen temperatures over 300 °C (Tice et al., 2004; Xie et al., 1997) and recrystallization and replacement are widespread (de Wit et al., 1982; Duchač & Hanor, 1987; Hanor & Duchač, 1990; Lowe et al., 1985; I. Paris et al., 1985). Alteration has widely stripped mobile cations from silicate minerals and infused

the rock with silica, potash, and, locally, carbonate (Duchač & Hanor, 1987; Hanor & Duchač, 1990; Lowe et al., 1985). Onverwacht sedimentary units were extensively silicified and now exist mainly as cherts (Lowe, 1999b), rocks composed largely of microcrystalline quartz with quartz domain size <35μm. BGB cherts commonly contain fine impurities including phyllosilicates, carbonates, iron oxides, and/or carbonaceous matter. Carbonates, mainly dolomite and/or ferroan dolomite, are also widespread as early cements and replacement materials. Most lithic grains and feldspars have been replaced by quartz-phyllosilicate mosaics, with sericite as the most common phyllosilicate in rocks or lithic grains that were originally felsic in composition and chlorite as a major alteration product of originally mafic volcanic materials. The main minerals to retain their original compositions are zircons, chromites, coarse quartz, barite, and some sulfides.

Fig Tree and Moodies sedimentary rocks and tuffs show less silica replacement than Onverwacht units and are mostly recrystallized aggregates of intergrown microquartz and fine phyllosilicates, including sericite and chlorite. Feldspars are locally well preserved. Although this alteration has been attributed to hydrothermal processes (de Wit et al., 1982; Duchač & Hanor, 1987; I. Paris et al., 1985), evidence suggests that much may represent widespread nearly syndepositional alteration resulting from the interaction of surface rocks and freshly deposited sediments with sea water (Hessler & Lowe, 2006; Lowe, 1999b).

In modern sedimentary systems, the composition of the main sandstone framework grains, termed QFL analysis for detrital quartz (Q), feldspar (F), and lithic grains (L), is a useful indicator of sediment provenance and the tectonic setting of sources and basins (Dickinson, 1970, 1985; Dickinson & Suczek, 1979; Ingersoll et al., 1984). Sandstones in the Archean BGB offer particular challenges to conventional QFL and petrographic analysis because of the pervasive post-depositional alteration, recrystallization, and metasomatism described above. Because of feldspar alteration, BGB sandstones often plot along the QL line in triangular QFL diagrams, even where the original rocks were feldspar-bearing, such as felsic volcanic rocks.

The extensive silica replacement and silica cementation of sedimentary and volcanic rocks throughout the BGB has made chert one of the most abundant sedimentary rocks in the Onverwacht Group, and the refractory character of chert grains to weathering has resulted in chert being one of the most abundant detrital grain types in sandstones of the Fig Tree and Moodies Groups (fig. 5). We will elaborate briefly on chert in detrital grains because it is so abundant but, in point counts, chert counts among neither the most weathering resistant (Qm) nor the most weathering-susceptible (as Lv and Ls) grain types. It is therefore useful as an aide in estimating sandstone provenance, transport, and depositional history. Many detrital chert grains in BGB sandstones are simple structureless aggregates of fine- microcrystalline quartz (fig. 5). However, many show a variety of internal quartz-domain shapes, sizes, size-mixtures, extinction patterns, and admixed impurities that result in distinctive petrographic grain types. These include homogeneous uniform microcrystalline quartz, microcrystalline quartz showing a range in sizes of the quartz domains, microcrystalline quartz exhibiting relict sweeping aggregate extinction suggesting formation by recrystallization of chalcedony, and chert showing concentric or layered variations in grain size suggesting formation as cavity fill. Carbonaceous chert containing black, opaque carbonaceous matter (fig. 5E, F) is common both as layers within the Onverwacht Group and as detrital grains in the Fig Tree and Moodies Groups (Lowe, 1999b). It includes a number of distinctive petrographic varieties: black opaque carbonaceous chert, chert containing fine carbonaceous matter dispersed in a translucent microquartz matrix, microcrystalline quartz containing blocky to rounded detrital carbonaceous particles, and microquartz containing fine flat to undulating carbonaceous laminations resembling microbial mats (fig. 5E, F). The varieties of carbonaceous chert particles in Fig Tree and Moodies sandstones include most of the varieties of carbonaceous chert seen in chert beds within the underlying stratigraphic sequence, especially the Mendon Formation and the Buck Reef Chert of the Kromberg Formation (fig. 2) (Tice & Lowe, 2006; Walsh, 1989; Walsh & Lowe, 1999). In detrital sediments of the Fig Tree and Moodies Groups in the ECD, the abundance and types of chert grains and carbonaceous grain types appear to reflect their different susceptibilities to weathering and distance of transport. More juvenile sandstones contain a wide variety of chert and carbonaceous grain types, including laminated carbonaceous chert, whereas more extensively weathered and transported sediments show few carbonaceous grains, mainly carbonaceous grains with fine, diffuse carbonaceous matter, and largely lack clotted carbonaceous matter and fine, mat-like laminations. Fig Tree sandstones tend to display a wide variety of carbonaceous grain types, including those showing mat-like carbonaceous laminations and complex detrital textures, while sandstones of the Moodies Group show sparse carbonaceous chert grains containing mainly simple dispersed carbonaceous matter.

3. METHODOLOGY

The present study is based on field mapping and stratigraphic studies by the authors and MS or PhD studies by Heubeck (1993), Zentner (2014), Harrington (2017), Drabon (2018), and Stoll (2020). Accurate stratal thicknesses are problematic throughout the study area, especially in thinly bedded shale and banded ferruginous chert sections, which commonly show complex, small-scale folding. We have estimated the total thickness of strata on the limbs of the larger folds both by measuring in the field and/or by calculating thicknesses from map distributions and measured strike and dips.

Thin sections prepared from sandstone samples served as the basis of petrographic analysis using the Gazzi-Dickinson method with a minimum of 300 counted framework grains per thin section (Dickinson, 1970; Dickinson & Suczek, 1979; Ingersoll et al., 1984).

Mudstone samples were analyzed for major and trace elements and REE at Washington State Peter Hooper Geo-

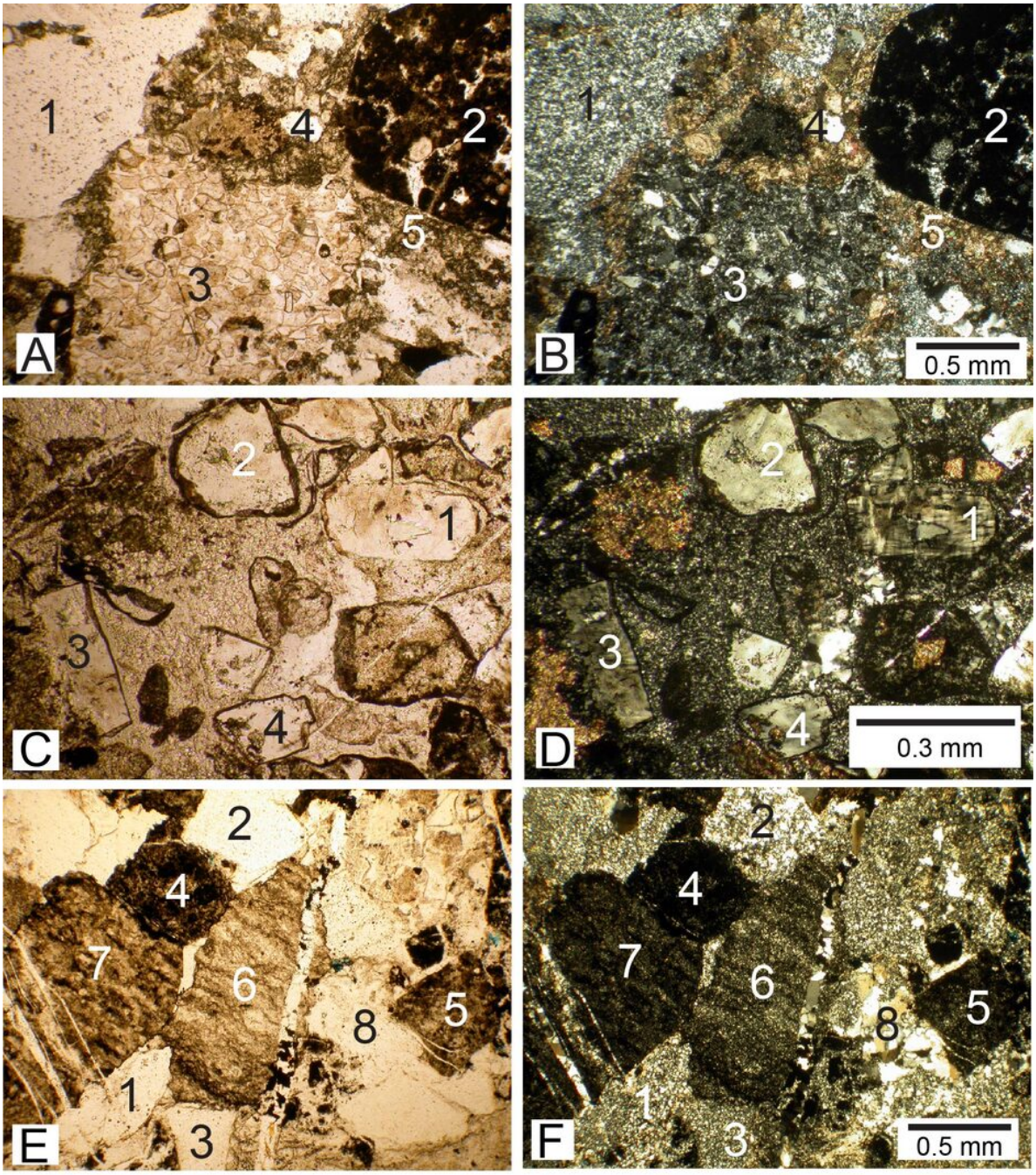

Figure 5. Photomicrographs of low-Qm Fig Tree sandstones in the Manzimnyama and Paulus Synclines, ECD. (A & B, plane light and crossed nicols, respectively). Sample BARB4-115.42 (BARB4 core depth in meters). The rock from the Gelegela Grit is dominated by a variety of chert grains including nearly pure microquartz (1) and others of carbonaceous chert (2). (3) is a lithic grain of well-sorted, fine-grained volcaniclastic sandstone common in the Gelegela Grit, now composed mostly of chert containing fine detrital quartz and feldspar, best seen under crossed nicols (B). Coarse detrital quartz (Qm) grains (4) make-up <1% of the rock. The matrix includes abundant high-relief, high-birefringence, very fine-grained carbonate (5). (C & D, plane light and crossed nicols, respectively). Sample BARB4-145.6 (BARB4 core depth, meters). This section is cut from a pebble of volcaniclastic sandstone composed largely of altered lithic grains but including a large component of feldspar. Grains 1–4 are feldspar all showing microcline grid twinning, best seen in grain 1 in (D). (E & F, crossed nicols and plane light, respectively). Sample (JH10-1 of Harrington, 2017) from the upper part of the Fig Tree Group in the southern Paulus Syncline with less than 1% Qm dominated by varieties of pure chert grains (1, 2, 3) as well as carbonaceous chert (4, 5, 6, 7) showing crudely layered (7), laminated (6), and massive to clotted (4, 5) textures. (8) is a small chunk of polycrystalline quartz possibly representing cavity fill. Another grain of lithic sandstone can be seen in the upper right corner.

Analytical Lab using a Thermo-ARL automated X-ray fluorescence spectrometer (XRF) and an Agilent inductively coupled plasma mass spectrometer (ICP-MS). The results are used herein for geochemical comparisons of samples and source terrain analysis.

Selected sandstone samples have been analyzed for detrital zircon geochronology using preparation techniques outlined in Drabon, Galić et al. (2019). $^{206}Pb/^{207}Pb$ ages were measured by Laser-Ablation Inductively Coupled Plasma Mass Spectrometry (LA-ICP-MS) with a 20 µm spot diameter at the Arizona LaserChron Center using the techniques discussed in Gehrels et al. (2008) and Gehrels and Pecha (2014). Grains with ^{204}Pb > 600 counts, low $^{206}Pb/^{204}Pb$, poor precision, U abundance above 400 ppm, or concordance below 95% were excluded. All but one of the ages discussed here, the age on the Manzimnyama Jaspilite in the Manzimnyama Syncline, have been reported and discussed previously (Drabon & Lowe, 2022; Stoll et al., 2021).

Cathodoluminescence analysis of quartz in selected polished thin sections was conducted by Byerly at the Stanford Mineral and Microchemical Analysis Facility using the JEOL JXA-8230 "SuperProbe" using the "xCLENT III" advanced hyperspectral CL system following the methodology outlined in Lowe and Byerly (2020).

4. STRATIGRAPHY AND SEDIMENTOLOGY OF THE EAST-CENTRAL DOMAIN

4.1. Onverwacht Group

In the studied part of the ECD, the Onverwacht Group is exposed mainly in narrow, sheared anticlines separating broader synclines of Fig Tree strata (fig. 3). The Onverwacht units include altered komatiitic volcanic rocks of the Mendon Formation, black and banded cherts at the top of the Mendon Formation, and, in the southeasternmost part of the study area, older basalts and associated sedimentary units of the Kromberg Formation. These rocks were not the focus of this study.

4.2. Fig Tree Group

4.2.1. MANZIMNYAMA AND MLUMATI SYNCLINES

Stratigraphy: The Manzimnyama Syncline is an asymmetric, northwest verging, overturned syncline that outcrops for about 8 km along strike in the northwestern ECD (fig. 3). The stratigraphy of rocks in the Manzimnyama Syncline, partially mapped by Heinrichs (1980) and subsequently by Heubeck (1993) and Lowe et al. (2012), was discussed and updated by Zentner (2014), Drabon, Galić et al. (2019), and Stoll et al. (2021), and is shown in a slightly modified version in figure 6, column B. ICDP Well BARB4 (Arndt et al., 2012) was drilled in the upright, east-dipping northwestern limb of the Manzimnyama Syncline and intersected rocks from the middle part of the Gelegela Grit to the base of the formation and into the cherts and serpentinized komatiites of the underlying Mendon Formation. The Manzimnyama Syncline is transected by the R40 road along which excellent exposures exist, although the rocks are extensively forested away from this highway. Nearly bedding-parallel faults cut rocks in the syncline, including faults in BARB4 near the Onverwacht-Fig Tree contact and, in outcrop, near the base of the Fig Tree Group and near the contact between the Manzimnyama Jaspilite and the overlying Gelegela Grit. The section shown in figure 6 combines information from BARB4, outcrops on the west limb along the R40 where the upper part of the Gelegela Grit and overlying units are well exposed, and from the sections on the east limb where the lower part of the section is well exposed and less affected by faults. We estimate that the total thickness of Fig Tree rocks preserved in the Manzimnyama Syncline is about 650 m with no top exposed (fig. 6, column B).

The Mlumati Syncline is a small syncline located between the Manzimnyama Syncline and The Heights Syncline (fig. 3). It has been studied and mapped by Stoll (2020) and (Stoll et al., 2021) and includes a section of rocks very similar in thickness, lithology, and depositional environments to those in the Manzimnyama Syncline (fig. 6, column A). In both synclines, the lower 5–20 m consists of light-gray-weathering, water-worked, felsic, tuffaceous strata of the Loenen member. The overlying section in both synclines is dominated by banded ferruginous chert (BFC) and banded iron formation (BIF) containing a few thin shale layers, sparse sandstone beds, and rare beds up to about 10 m thick of chert-plate breccia. The BFC consists of interlayered bands from less than 1 to ~10 cm-thick of white chert or, more rarely, jasper (red hematitic chert), siderite (mostly weathered to iron oxide at the surface), and greatly subordinate shale. BIF in these synclines is composed of alternating bands of jasper, hematite, and siderite.

In the Manzimnyama Syncline, the Schoonoord member, 50–100 m thick, overlies the Loenen member (fig. 6). It is composed mainly of BFC with sporadic shale and sandstone beds, chert-plate breccias, and BIF zones. It is overlain by the Manzimnyama Jaspilite that includes Lower and Upper Jaspilite members, about 140 and 50+ meters thick, respectively, separated by the 350 m-thick turbiditic sandstones of the Gelegela Grit (fig. 6).

In the Mlumati Syncline, rocks above the Loenen member consist largely of BFC with thin, interbedded units of BIF and one prominent 20–30 m-thick unit of lithic sandstone that Stoll et al. (2021) correlated with the Gelegela Grit (fig. 6).

Sedimentology: All Fig Tree rocks in the Manzimnyama and Mlumati Synclines reflect sedimentation in relatively deep water, well below wave base and outside of any zones influenced by waves, tides, or significant current activity other than turbidity currents. The overall setting was quiet with passive sedimentation of precipitative iron-rich sediments and the settling of fine hemipelagic mud, although, overall, mudstone and shale constitute a small part of the Fig Tree section. The chert-plate breccias mark episodes of submarine sliding and soft-sediment flowage.

The Gelegela Grit represents a major episode of sand influx into the basin via turbidity currents. We detected no major grain size or bed-thickness trends in the Grit except for the localization of the few pebble conglomerates toward its top along the R40. The tabular nature of the

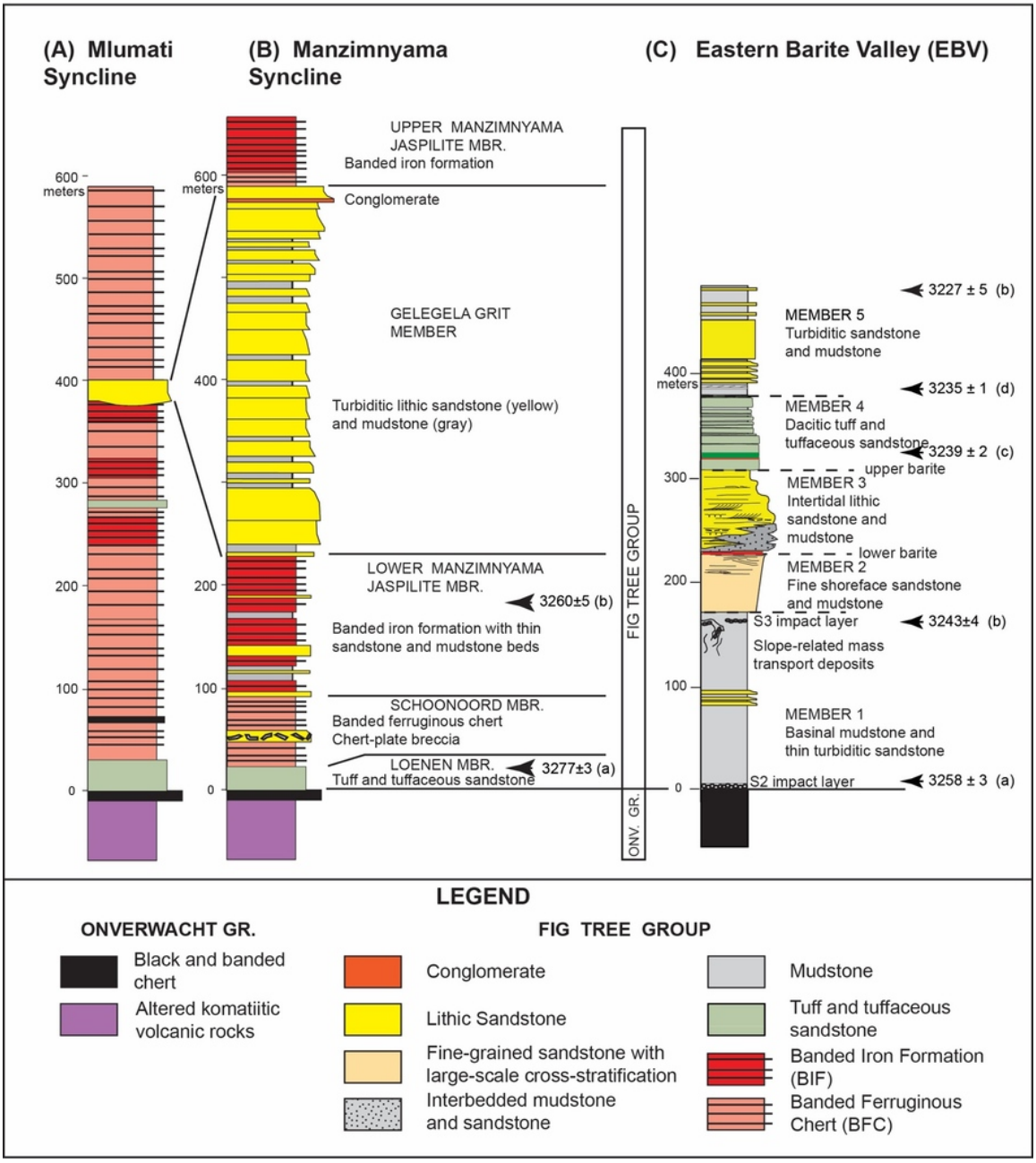

Figure 6. Stratigraphic columns of uppermost Onverwacht Group and Fig Tree Group in the Mlumati and Manzimnyama Synclines and Eastern Barite Valley (EBV). (A) Mlumati Syncline from Stoll et al. (2021). (B) Composite stratigraphic column of Fig Tree rocks in the Manzimnyama Syncline along R40 and in ICDP drill core BARB4. Stratigraphic units modified from Heinrichs (1980), Zentner (2014), and Stoll et al. (2021). References for ages: (a) Drabon, Galić et al. (2019). Stoll et al. (2021) report a similar age of about 3,280 Ma for detrital zircons separated from three samples of the Loenen member in the Mlumati Syncline; (b) Present study, a thin tuff in the Manzimnyama Jaspilite on the east limb of Manzimnyama Syncline. The five concordant zircons separated from this tuff yielded a SHRIMP age of 3.260±0.005 Ga. (C) Stratigraphic column of rocks in the Eastern Barite Valley showing the major stratigraphic divisions and inferred settings of deposition (modified from Drabon, Heubeck, et al., 2019 and Lowe et al., 2019). The rocks show an initial period nearly 15 myr long of fine-grained, quiet-water mud sedimentation. The progradation of a fan-delta and shallow-water section was initiated immediately following the S3 impact at ~3243 Ma. This interval of shallow-water and fan delta deposition lasted for about 4 myr before the return of quiet water, subaqueous, largely fine-grained sedimentation. This overall cycle of sedimentation is characteristic of Fig Tree deposits in most areas in the BGB. References for ages in myr: (a) Byerly et al. (1996); (b) Kröner et al. (1991); (c and d) Drabon, Galić et al. (2019). In spite of their very different ages, all sections show an early stage of quiet, possibly deep-water sedimentation followed by the influx of coarse siliciclastic terrigenous sediments and a closing interval of fine, quiet-water sedimentation.

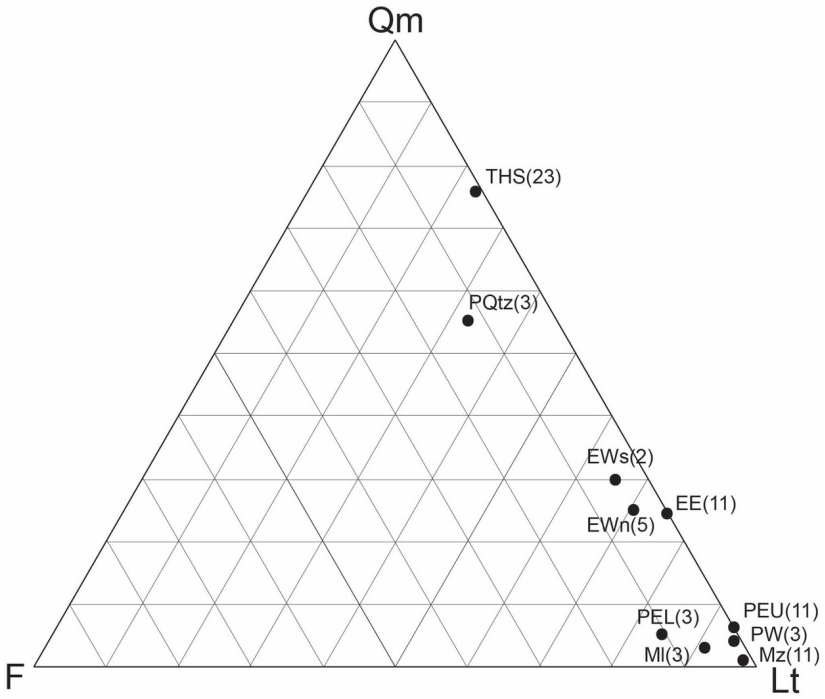

Figure 7. QmFLt plot for the Manzimnyama, Paulus, and Emlembe Belts in the ECD and the Moodies Group in The Heights Syncline. Each point represents an average of several thin section point counts, the number of thin sections in each indicated in parentheses. Locations: Mz, Manzimnyama Syncline; Ml, Mlumati Syncline; PW, west limb of the Paulus Syncline; PEL, lower east limb of the Paulus Syncline, PQtz., quartz-rich middle unit in the east limb of the Paulus Syncline; PEU, upper part of the east limb of the Paulus Syncline; EE, eastern arm of the Emlembe Belt; EWn, western arm of the Emlembe Belt, north of the BB Road; EWs, western arm of the Emlembe Belt, south of the R40 road; THS, Moodies Group in The Heights Syncline. Data for Manzimnyama Syncline from Drabon et al. (2017) and Stoll et al. (2021); Mlumati Syncline from Stoll (2020); Paulus Syncline and Emlembe Belt from Harrington (2017); Moodies Group from Heubeck (1993).

sandstone beds in outcrop along the R40, the dominance of massive suspended-sediment fallout layers from collapsing high density turbidity currents like those described as S3 divisions by Lowe (1982), the paucity of scour and erosion features, and paucity of T_b flat-lamination and T_c cross-lamination suggests that the Gelegela Grit was deposited by collapsing high-density turbidity currents, possibly as part of a large basin-floor sand lobe or frontal splay. We saw little cross-bedding or other features that would allow determination of paleo-flow direction.

Petrography: Modal analysis of sandstones in the Manzimnyama and Mlumati Synclines has been discussed by Drabon, Galić et al. (2019), Stoll et al. (2021), and Zentner (2014). All sandstone beds are composed of lithic sandstone containing < 3% coarse, monocrystalline quartz (Qm of Dickinson, 1970; Dickinson & Suczek, 1979) (figs. 5 & 7). Coarse, monocrystalline quartz (Qm) includes a few (<1%) grains of simple coarse monocrystalline quartz: perhaps half of the coarse quartz is in polycrystalline grains that show layering or comb-structure indicating an origin as vein- or cavity-fill quartz. Rare euhedral beta (volcanic) quartz is also present. Some coarser grains show a relict fibrous structure and represent chunks of recrystallized chalcedony.

Many sand-sized grains are composed of relatively pure chert (fig. 5), carbonaceous chert (fig. 5A, B, E, F), or chert with iron oxide or phyllosilicate impurities. Grains of silicified fine- grained lithic sandstone also containing a small amount of fine monocrystalline quartz are present in many samples (fig. 5A, B). Sericite rather than chlorite is the dominant phyllosilicate in altered lithic grains suggesting that they were originally more felsic grains. Other rock fragments represent volcanic rocks with plagioclase as phenocrysts and/or microlites. Quartz-chlorite grains are rare but in the upper half of the Gelegela Grit, chamosite, $(Fe^{2+}, Mg)_5Al_2Si_3O_{10}(OH)_8$, is present as rounded, often crushed detrital grains in the sandy turbidites.

Feldspar makes up <3% of sandstone samples. In the Gelegela Grit feldspars are also not uncommon within volcanic rock fragments (fig. 5A, B, C, D). Some clasts of volcaniclastic sandstone contain abundant, well-preserved microcline grains showing characteristic grid twinning (fig. 5C, D) and idiomorphic shapes suggesting that they represent volcanic phenocrysts, probably plagioclase, that have been replaced by microcline, as described from member H6 of the Hooggenoeg Formation (Lowe & Byerly, 2020).

Shale geochemistry: Geochemical analyses of Fig Tree shale samples from the Manzimnyama and Mlumati Synclines (Drabon, Galić, et al., 2019; Stoll et al., 2021; Zentner, 2014) (fig. 8) show that there is a tendency toward an up-section shift in the average composition of the inferred source rocks. The Loenen felsic ash represents the

primary source near the base of the Fig Tree Group but upward, sources become progressively more mafic until shales in the Gelegela Grit show compositions suggesting a mixed felsic-basaltic or felsic-komatiitic source. The Cr values of shales within the Gelegela Grit is uniformly above 1000 ppm and commonly above 2000 ppm, suggesting that the source rocks included komatiites.

Zircon geochronology: The results of detrital zircon age analyses of Fig Tree sandstones in the Manzimnyama and Mlumati Synclines have been discussed by Drabon et al. (2017), Drabon and Lowe (2022), and Stoll et al. (2021). They show overwhelming derivation of the detrital zircons from rocks 3.42–3.45 Ga, the age of felsic rocks in H6 of the Hooggenoeg Formation, with a greatly subordinate mode at 3.275–3.295 Ga representing ages equivalent to the upper part of the Mendon Formation. Fig Tree sources are not well represented in detrital zircons in Fig Tree strata in the Manzimnyama and Mlumati Synclines. We here report a zircon age from a thin felsic tuff in the Lower Manzimnyama Jaspilite member on the east limb of the Manzimnyama Syncline (25°54.5'S., 31°06.2E.). Zircons separated from this tuff were dated by Byerly using the Stanford SHRIMP and yielded a mean age among the 5 zircons dated of 3.260±0.005 Ga.

Provenance: All provenance indicators that we have examined are consistent with derivation of Fig Tree sandstones and shales in the Manzimnyama and Mlumati Synclines from three main sources: (1) early felsic eruptive materials probably represented at least in part by ~3.277 Ga tuffs of the Loenen Formation at the base of the unit (Drabon, Galić, et al., 2019; Stoll et al., 2021) but also including slightly older felsic rocks, 3.28 to 3.30 Ga; (2) H6-age felsic volcanic rocks, ~3.42–3.45 Ga, which contributed the bulk of the zircons and probably felsic lithic grains and observed volcanic pebbles and feldspars in the Gelegela Grit; and (3) mafic to komatiitic volcanic rocks and associated cherts, probably the volcanic-sedimentary units of the underlying Mendon Formation. Shales record an upward transition from rhyolitic-sourced sediments near the base to mafic to komatiitic sources in the Gelegela Grit. The Gelegela Grit is interesting because the coarser sediments reflect mainly felsic sources and the shales mafic to komatiitic sources. The former is represented by feldspar-bearing porphyritic rock fragments in some of the coarser sandstones and conglomerates, by microquartz-sericite rock fragments in the sandstones, and by H6-age detrital zircons.

Fig Tree sedimentary rocks in the Manzimnyama and Mlumati Synclines reflect relatively deep-water, basinal, marine sedimentation dominated by chemical processes of precipitation within the water column and sparse fine hemipelagic deposition of shales punctuated in the upper parts of the sections by the influx of lithic sandy debris transported by turbidity currents. The sandy lithic components of this debris were derived mainly from cherts of the Mendon Formation and quartz-poor felsic volcanic rocks H6 in age and 3.27–3.29 Ga volcanic sources. The fine-grained muddy components appear to have been derived mainly from weathering of mafic and ultramafic volcanic rocks of the Mendon Formation.

4.2.2. PAULUS SYNCLINE

Stratigraphy: The Paulus Syncline lies to the southeast of the Manzimnyama Syncline across a narrow belt of sheared altered komatiite and chert termed the Schoonoord Anticline (fig. 3). Previously, the Paulus Syncline was thought to be divided by faults into three structural and stratigraphic subdivisions termed the north, central, and south Paulus Syncline (Drabon & Lowe, 2022; Harrington, 2017; Stoll et al., 2021). This subdivision was based in part on the presence of 30 meters of quartz-rich sandstone mapped as Moodies Group by Lowe et al. (2012) between the Paulus south and Paulus central sections. However, mapping in 2022 by the authors confirmed previous mapping by Heubeck (1993) that shows that this sandstone is within the Fig Tree Group and can be traced as a series of discontinuous lenses around the Paulus Syncline on both limbs (fig. 4). We here regard the Paulus Syncline as a largely intact structure.

Stratigraphic columns of the northwest and southeast limbs of the Paulus Syncline are shown in figure 9. On the northwest limb, the Fig Tree-Onverwacht contact is well exposed along the R40 adjacent to the Schoonoord Anticline, where a 2–4 m-thick unit of gray cherty sedimentary rock marking the top of the Mendon Formation is overlain by about 3 meters of sandy rocks of the Fig Tree Group probably representing the Loenen member. This is succeeded by a complexly folded section of thin-bedded mudstone and BFC with an indeterminate thickness but probably no less than 50 m. The rock overlying this BFC is poorly exposed along the BB Road but includes laterally a lens of BIF, probably <10 m thick, representing the Manzimnyama Jaspilite, succeeded by about 500 m of largely mudstone overlain by a section of interbedded conglomerate and mudstone (fig. 9). Along the R40, no prominent sandstone or conglomerate units are seen in this mudstone section but just west of the road in the hinge of the Paulus Syncline the Fig Tree includes thick lenses of chert-clast conglomerate and a zone of thin-bedded mudstone and quartz-rich sandstone about 10 m thick (figs. 4 & 9).

On the northwest limb of the Paulus Syncline, conglomerate about 550–600 m above the base (fig. 9) has a sharp lower contact with underlying shales that may be erosive, but no clear scour or truncation features were seen in outcrop. This conglomerate, about 10–20 m thick, thins and lenses out to the southwest along strike, is well layered, and includes a distinctive type of conglomerate in which the clasts are very tightly packed, lacking a sandy matrix (fig. 10A). The composition of this conglomerate varies from place to place, including some in which blocky clasts are composed largely of banded chert probably derived from BFC (fig. 10A) and other layers composed mainly of rounded clasts of gray chert. Sandstone showing large-scale cross-stratification is present in the upper part of this conglomerate (fig. 10B). Above this conglomerate is a mudstone layer and then at least one and possible several additional units of pebble to cobble conglomerate interbedded with shale.

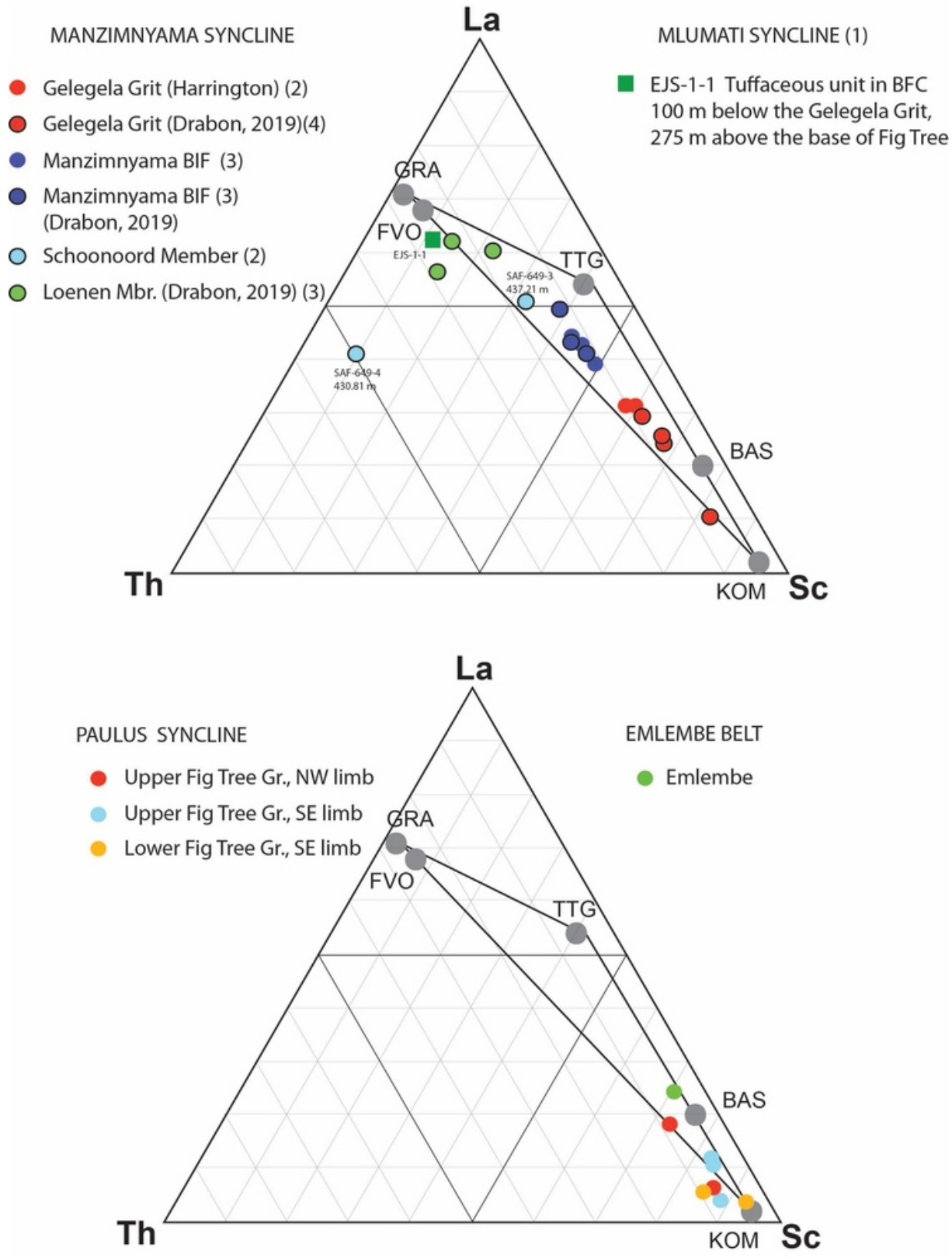

Figure 8. Immobile element Sc-La-Th plots of shales of the Fig Tree Group in the ECD and representative analyses of potential source rocks (KOM: komatiite; BAS: tholeiitic basalt; TTG: tonalite-trondhjemite-granodioritic plutons; GRA: granite; FVO; felsic volcanic rocks). The results show the felsic influences on the lowest shales in the Manzimnyama Syncline and the increasing importance of mafic and komatiitic sources upward. Data from Condie and Hunter (1976), Zentner (2014), Harrington (2017), Drabon, Galić et al. (2019), Stoll (2020), Stoll et al. (2021).

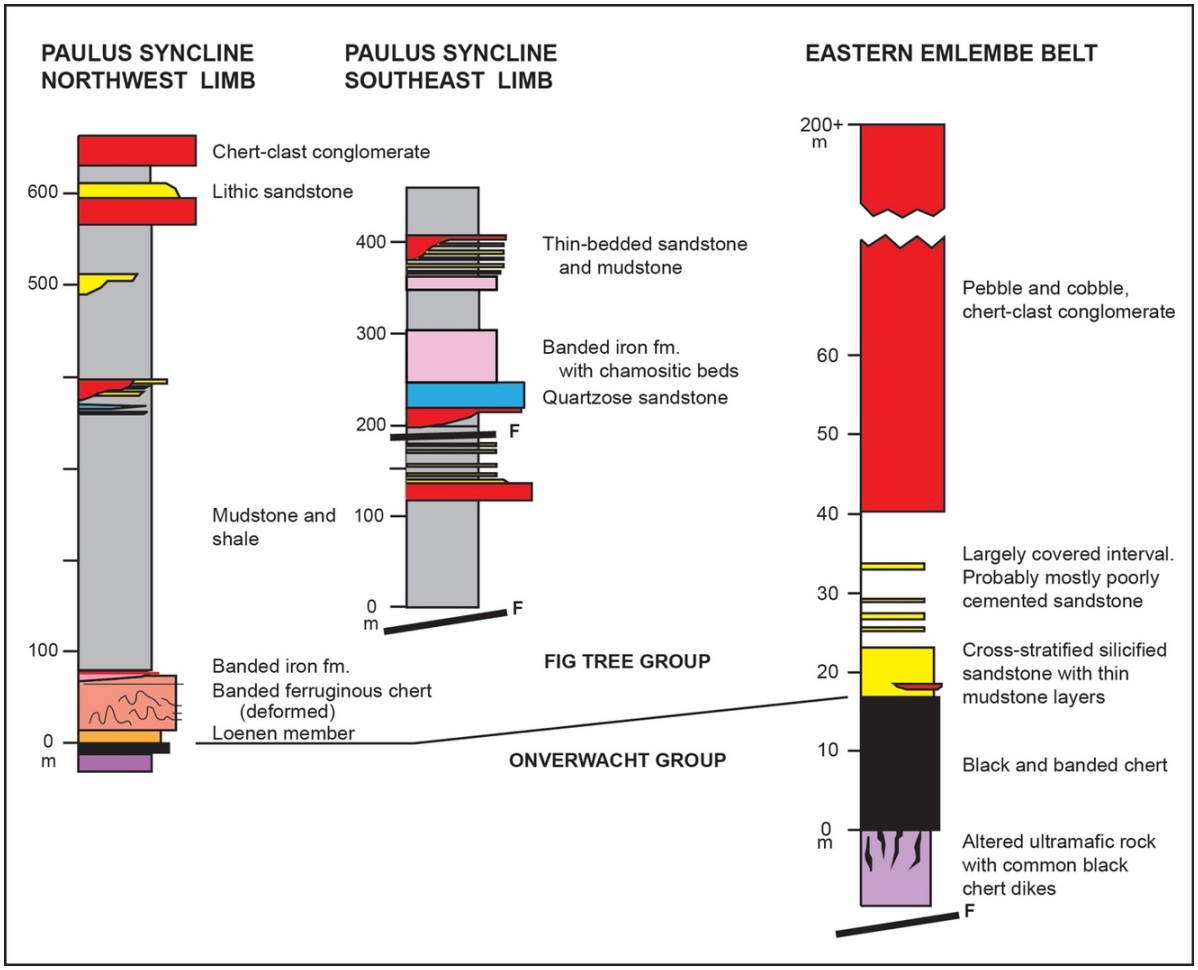

Figure 9. Stratigraphic columns of Fig Tree rocks on the northwest and southeast limbs of the Paulus Syncline along the R40 and in the eastern Emlembe Belt at locality C, figure 4. Note differences in scale among the columns.

These beds are close to the hinge of the Paulus Syncline and the stratigraphic sequence above this point is uncertain. The contrasting compositions of closely spaced conglomerates suggest local sources of debris and the dominance of conglomerate and paucity of sand and sandstone suggest derivation from rocks that weathered to yield little sand-sized material.

The Fig Tree section on the southeast limb of the Paulus Syncline is well exposed along and adjacent to R40. From base to top it can be split into five subdivisions (fig. 9): (1) a basal unit of mudstone of which only the uppermost 100–150 m is exposed; (2) a 100± m thick section of mudstone with a prominent lenticular unit 10–15 m thick of conglomerate at the base, interbedded thin-bedded sandstone and mudstone in the middle and a prominent channel-fill conglomerate at the top (fig. 11A); (3) 30 m of quartzose sandstone (fig. 11A); (4) a section 150+ m thick, dominated by iron-rich units including BIF and chamositic sandstones, shale, and lenticular beds of chert-clast conglomerate and sandstone up to about 30 m thick (fig. 11A), and (5) an upper section at least 50 m thick of mudstone. Along the R40, the basal mudstone is in contact on the southeast with a thick tectonic breccia composed of black chert blocks in a matrix of sheared, altered komatiitic volcanic rock (figs. 3 and 4). The stratigraphic base of the mudstone is not exposed along the R40 but about a kilometer to the southwest the mudstone overlies black and banded chert at the top of the Mendon Formation.

Above the basal mudstone along the R40, the section consists of a lenticular conglomerate overlain by interbedded mudstone and thin-bedded sandstone. The conglomerate matrix and sandstone layers are composed of sandstone with less than 10% Qm (fig. 7). The lower conglomerate is a chert-clast, pebble and cobble conglomerate about 10–15 m thick along R40 that contains a low-Qm (<10%) sandstone matrix and is succeeded by another thick mudstone section with thin sandstone beds (fig. 9). The topmost 2 to 4 meters of mudstone show a gradual upward increase in siderite and immediately below the overlying conglomerate is a 2 to 3-m-thick zone of very hard, reddish, siderite-cemented mudstone. This sideritic zone is cut by an erosive channel (fig. 11A) filled by poorly-sorted, chert-clast conglomerate with a low-Qm chert-arenite matrix (fig. 10C) that contains a low but distinctive (<3%) feldspar content. The clasts range from rounded to angular but are overall more angular, distinctly poorly sorted, and made up largely of black chert, lacking the diversity of chert clasts seen in many other conglomerates. There is an absence of cross-

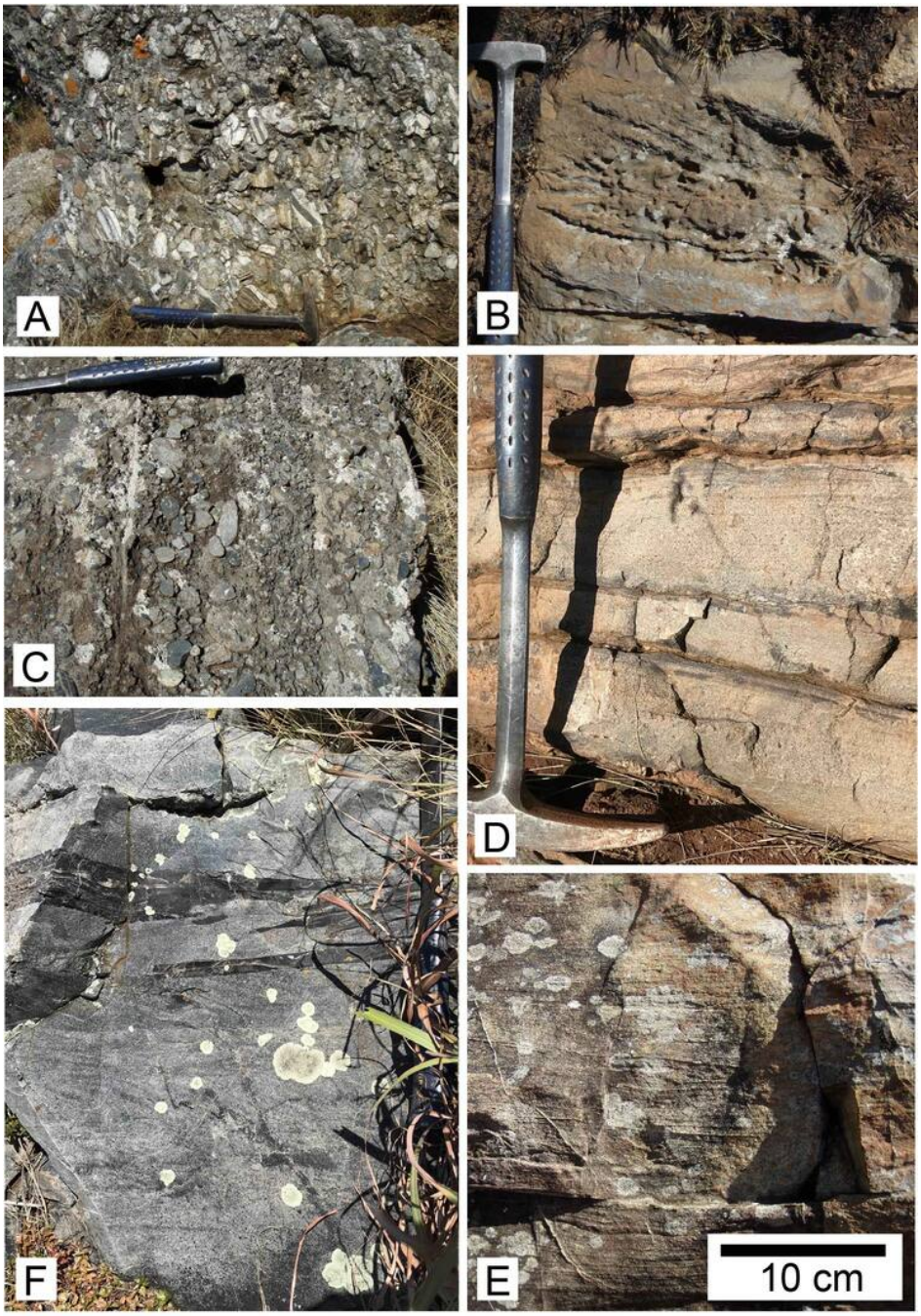

Figure 10. Sedimentary features of Fig Tree Group rocks in the Paulus Syncline and Emlembe Belt. (A) Tightly packed conglomerate composed largely of tabular clasts of banded chert on the northwest limb of the Paulus Syncline. The narrow range of clast compositions and lack of a sandy matrix suggest very local derivation of debris. (B) Large-scale cross-stratification in sandstone at the top of the lowest major conglomerate unit in the upper part of the Fig Tree Group on the northwest limb of the Paulus Syncline. Cross-stratification like this is rare. (C) Well-bedded, gray to black chert-clast, channel-fill conglomerate with a carbonate-rich sandstone matrix near the middle of the Fig Tree Group, underlying the quartz-rich sandstone, southeast limb of Paulus Syncline (fig. 11A). (D) Thin-bedded quartzose (>50% Qm) sandstone from the middle of the Fig Tree Group, northwest limb of the Paulus Syncline. Beds are flat-laminated and some show cross-laminations at the top. These resemble deposits of surging currents, such as turbidity currents. (E) Current laminated chamosite-bearing sandstone from the upper part of the Fig Tree Group, southeast limb of Paulus Syncline. The fine-grained sandstone is dominated by flat, upper flow regime plane bedding and small sets of cross-lamination. (F) Cross-laminated sandstone (gray) with silicified mudstone lenses and layers (black) making up the lowest part of the Fig Tree group, eastern branch of Emlembe Belt (locality C, fig. 4). The mud-sand alternation suggests alternating current-active and quiet-water intervals. Geologic hammer (right) for scale.

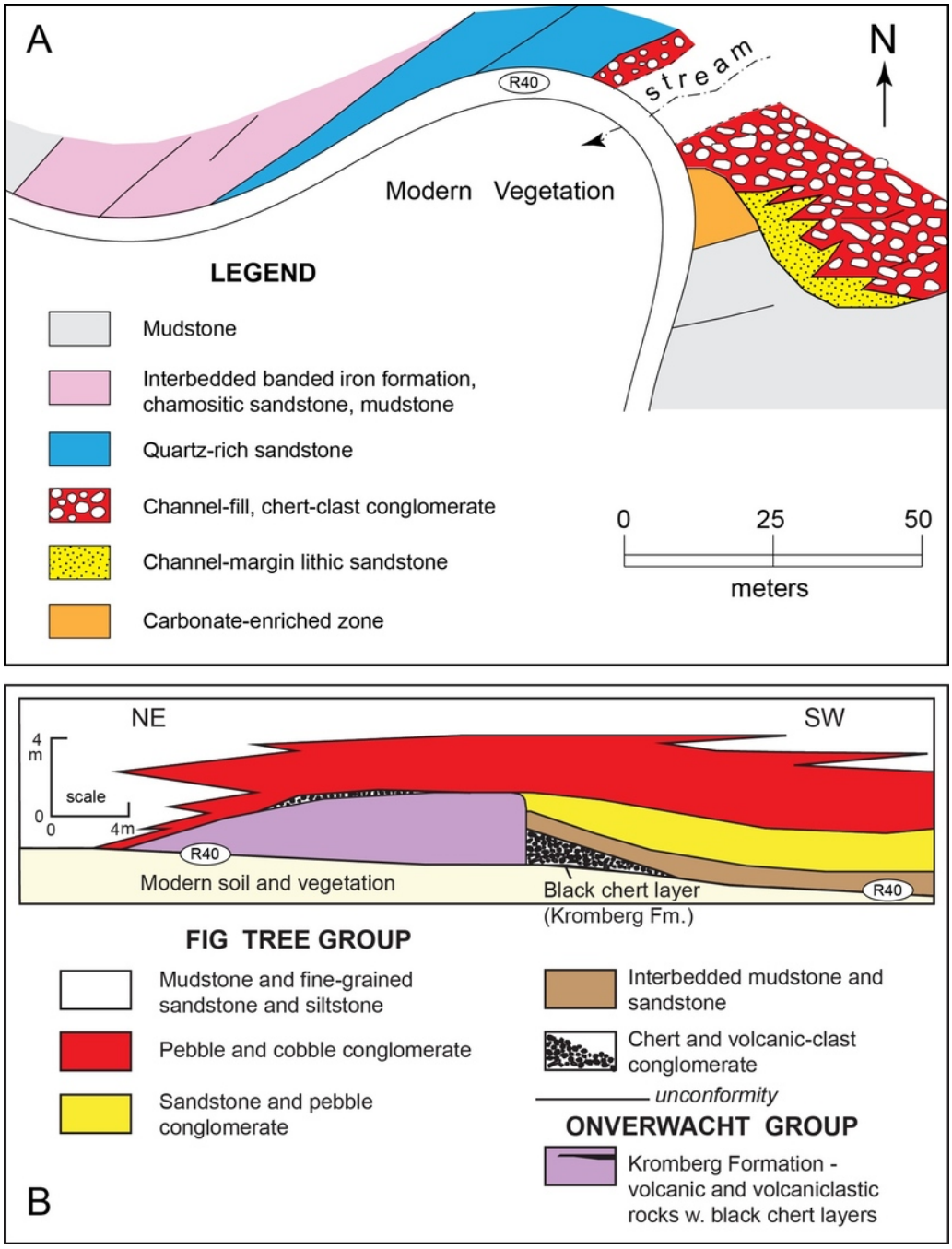

Figure 11. Geologic relationships of Fig Tree strata along the R40. (A) Geologic map of the middle part of the Fig Tree Group on the southeast limb of the Paulus Syncline. The section NE of the R40 road shows channel-fill conglomerate cut into an underlying mudstone that, outside of the channel along the road, shows increasing siderite content toward the contact. On the north side of the stream, the conglomeratic section is directly overlain by 30 m of quartzose sandstone. Stream crosses R40 road at 25° 55.676'S., 31° 06.272'E. (B) Sketch of the Onverwacht-Fig Tree contact in a vertical outcrop (locality B, fig. 4) along the R40 about 420 m NW of the Diepgezet junction, eastern Emlembe Belt. Basal strata of the Fig Tree Group, including black chert clast conglomerate, lie with erosional unconformity on volcanic rocks and black chert of the Kromberg Formation of the Onverwacht Group. Rocks below road level are not exposed.

bedding and systematic normal or inversely graded beds. The main structures are flat layering and local minor scour.

This chert-clast conglomerate is overlain along the R40 by a 30-m-thick unit of medium- to coarse-grained quartz-rich sandstone (fig. 11A) showing 50–60% monocrystalline quartz grains (fig. 7). This well-lithified, silica-cemented unit is crudely stratified but we have not seen cross-stratification and other primary current features in this unit because of the dark color and uniform silica cementation. The sand size and good sorting suggest that the sediment was current deposited. Around the hinge of the Paulus Syncline, the northernmost outcrop of this quartz-rich sand-

stone consists of stacked, mostly thin (<20 cm thick) sandstone beds that show internal structures suggesting deposition by currents of declining velocity, perhaps turbidity currents (fig. 10D).

The lower ~100 m of the section above the quartzose sandstone consists of banded iron formation, iron-rich shale, and interbedded units of fine-grained sandstone composed of about 50% siliciclastic detritus and 50% detrital chamosite grains. The chamosite and admixed chert grains locally form units up to a meter thick (fig. 10E). These units are not graded, are pervasively current structured, mainly with flat lamination and small-scale cross-lamination, and do not show an internal arrangement of structures suggesting deposition by turbidity currents. They appear to represent small bars or channels developed within an overall low-energy but current-active setting of deposition. A few coarser, lithic sandstone beds are present and thin jaspilite layers occur sporadically. The upper half of the iron-rich section is composed largely of BIF and shale. The top is marked by a 10–15 m thick zone of interbedded coarse sandstone with rare conglomerate and shale. Just west of the R40, this interval is a pebble to cobble conglomerate 20–30 m thick (fig. 9, southeast limb). Along the highway, the conglomerate has thinned to about 3 m thick. Uphill to the east of the road, the interval extends as a series of 0.5 to 1.5 m-thick sandstone beds, some with conglomeratic bases, interbedded with shale. We interpret this interval to represent a conglomerate-filled channel west of R40 that is replaced by the interval of thinner, probably overbank sandstone beds to the northeast of R40. This conglomerate is overlain by at least 50 m of fine, dark gray shale at the top of the exposed section.

Sedimentology: The lower part of Fig Tree rocks in the Paulus Syncline on both limbs is composed of banded ferruginous chert or mudstone with a few mainly thin, fine-grained sandstone beds. These units appear to represent quiet and possibly relatively deep-water conditions. No cross-stratification, cut-and-fill, or other suggestions of significant current activity were noted. The overlying zone of chert-clast conglomerate and quartzose sandstone lenses in the middle to upper part of the Fig Tree Group marks the influx of coarser clastic sediment from two distinctly different sources: one dominated by low-quartz (<10% Qm) chert clast conglomerate and sandstone and the other by medium- to fine-grained quartz-rich (>50% Qm) sandstone.

The low-Qm chert-clast conglomerate immediately underlying the quartz-rich sandstone along the BH Road on the southeast limb shows a pronounced erosional lower contact that cuts 10–15 m into and through the underlying siderite-enriched mudstone (fig. 11A). It is composed of poorly-sorted, rounded to angular cherty conglomerate and sandstone (fig. 10C). The siderite-rich zone below this conglomerate is a unique zone in our experience in the BGB. It represents a mudstone section that has been thoroughly infused with siderite and microcrystalline quartz. Its situation immediately below an erosional unconformity and a poorly-sorted conglomerate may suggest that it represents a zone of surface exposure and evaporative precipitation, perhaps resembling a caliche. Hessler et al. (2004) has described a weathering rind on alluvial pebbles in the Moodies Group that show similar enrichment in siderite. Another well-defined channel is present higher in the section (fig. 9) and we suggest that most of the lenticular sandstone and conglomerate lenses in these sections represent channel-fill units.

The upper part of the section on the southeast limb of the Paulus Syncline is an interesting iron-rich section that includes small, cross-laminated bodies of chamositic sandstone (fig. 10E) in a background of mudstone, jasper, and thin chert beds. This appears to represent an overall low-energy environment that was swept by frequent to continuous currents that worked and rippled available sand, much of which was chamosite. This was more like a quiet but shallow lagoon or shallow, open marine shelf in modern settings. Interbedded lenticular conglomerates appear to represent channels cutting across these lower-energy environments.

Petrography: All sandstones in the Paulus Syncline except the quartz-rich sandstone are composed largely of chert grains and altered microquartz-phyllosilicate lithic grains (fig. 7E, F). They include <10% Qm, including cavity-fill and vein polycrystalline quartz grains. Except in the low-Q conglomerate immediately underlying the quartz-rich sandstone along the BB Road, no feldspar or ferromagnesian silicate grains were seen.

In contrast, the quartz-rich sandstone beds near the middle of the Fig Tree Group are composed of >50% and up to 70% Qm, averaging 55–60% sand-sized, mostly monocrystalline quartz (figs. 7 & 12A, B) and contain 10–20% feldspar, including both potassium feldspar (fig. 12A, B) and plagioclase. This strongly bimodal character suggests that the sediments represent two very contrasting sources of sediment. Cathodoluminescence suggests that all of the quartz was derived from volcanic sources.

Shale Geochemistry: The geochemistry of shales collected from Fig Tree rocks in the Paulus Syncline are plotted in figure 8. All are from the upper part of the sequence and all show compositions consistent with mafic to komatiitic sources, including Cr levels from 1500 to 3000 ppm (Harrington, 2017).

Detrital zircon geochronology: DZ analyses are available from sandstones associated with conglomerates in the upper parts of the Paulus sections (Drabon et al., 2017; Drabon & Lowe, 2022; Harrington, 2017). All show two main age peaks at about 3.28–3.295 Ga and ~3.445 Ga, consistent with derivation from earliest Fig Tree or late Mendon and H6-age felsic rocks.

Provenance: The results of this study indicate quartz-poor, non-felsic sources for the bulk of the detrital sediments in the Fig Tree Group in the Paulus Syncline. Conglomerate and shale dominate over sandstone in virtually all sections, suggesting that coarse plutonic rocks were not exposed. There is a sandy unit at the base on the northeastern limb that we tentatively correlate with the felsic volcanic Loenen member. Shale samples from the upper half of the Fig Tree Group indicate mafic to komatiitic sources, suggesting that there is an overall upward increase in mafic to komatiitic sources of detrital material. These features

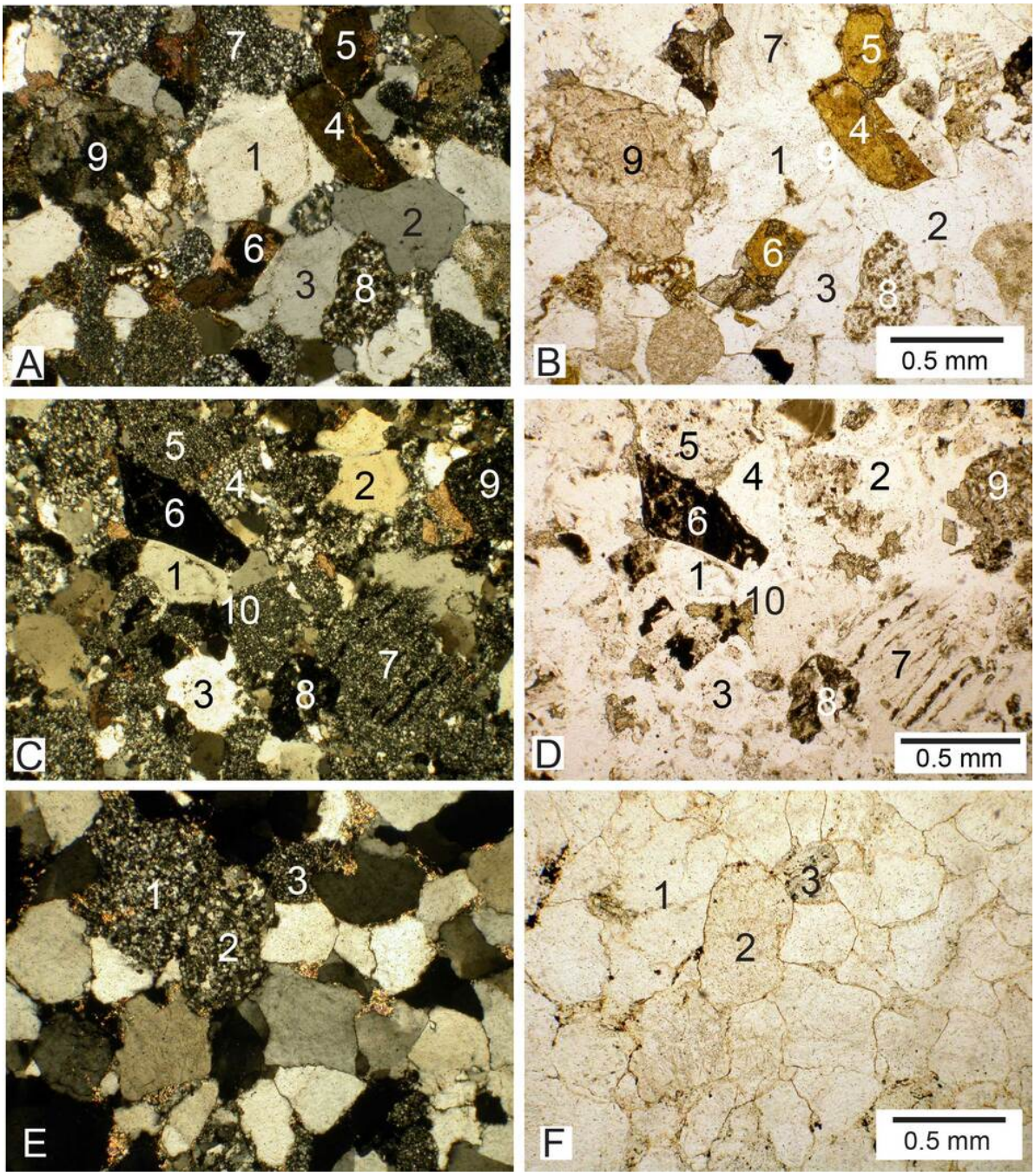

Figure 12. Photomicrographs of quartz-rich sandstones from the ECD. (A and B, crossed nicols and plane light, respectively). Sample SAF-6-63 from the quartz-rich (ave. 55–60% Qm) sandstone near middle of the Fig Tree Group on the southeast limb of the Paulus Syncline. Qm quartz grains, most showing syntaxial overgrowths (1, 2, and 3). Potassium feldspar grains are stained yellow (4, 5, 6). Chert grains (7, 8) are subordinate to Qm. (9) Grain of polycrystalline feldspar, possibly plagioclase. (C and D, crossed nicols and plane light, respectively). Sample JH11-2 from the eastern Emlembe Belt. Qm grains are prominent (1, 2, 3), most with overgrowths in optical continuity with the underlying grain. Grains of relatively pure chert (4, 5) are mixed with carbonaceous chert grains (6 thru 9) including a few composed of laminated chert and carbonaceous matter (7). (10) is a small altered volcanic gain composed of chlorite and opaque matter. (E and F, crossed nicols and plane light, respectively). Moodies Group in The Heights Syncline. Well-sorted, medium- to coarse-grained quartzose sandstone (>60% Qm) with a subordinate population of chert grains (1, 2, and 3), most of which lack carbonaceous matter.

and the chert-rich sandstones and conglomerates suggest that most Fig Tree detritus was derived from older Fig Tree rocks or from the Mendon Formation or equivalent rocks.

The exception are the quartz-rich sandstones near the middle of the Fig Tree Group. These point to a quartz-bearing source that was probably extensively weathered

to produce such abundant quartz. This quartz-rich sandstone lacks admixed gravel-sized clasts and interbedded conglomerate. It represents a distinct source of debris that was not extensively mixed with sand from the chert-dominated sources before deposition. CL studies suggest that the source was volcanic rocks.

4.2.3. EMLEMBE BELT

Stratigraphy. Coarse conglomerate and quartz-bearing (10–50% Qm) sandstone units in the eastern part of the ECD are here assigned to a single structural belt named for the highpoint, Emlembe (fig. 1), on the ridge along the east side of the area that overlooks Eswatini (Swaziland). The summit of Emlembe at an elevation of 1861 m forms Eswatini's highest peak and also lies at a bend in the international border (fig. 1). Heubeck (1993) and Lowe et al. (2012) mapped what we are terming the Emlembe Belt as including both Fig Tree and Moodies rocks. The Moodies component was shown as a complex synclinal structure that Stoll et al. (2021) termed it the Emlembe Syncline but the internal stratigraphy and younging directions are sufficiently poorly constrained that we have not been able to verify the synclinal nature of this belt. The Emlembe Belt in the study area (fig. 4) includes two branches, the eastern and western branches, separated by a belt of basaltic volcanic rocks of the Kromberg Formation (figs. 3 & 4). The Kromberg volcanic units wedge out structurally between the western and eastern Emlembe belts just north of the R40 (fig. 4).

Both Emlembe Belt branches (fig. 4) are composed of structurally complex pebble to cobble conglomerate and coarse- to medium-grained sandstone. The sandstones and the sandstone matrices to the conglomerates are distinctive because of the high (10–50%) content of coarse monocrystalline quartz (Qm) as well as coarse polycrystalline (Qp) quartz (not including chert) (fig. 7). Mudstone is sparse and, outside of rare roadcuts, largely covered at the surface. At least two or three hundred meters of strata are present, but we have been unable to establish an internal stratigraphy because of the structural complexity, lack of distinctive stratigraphic markers, and paucity of top indicators. There is widespread interfingering of conglomerate and sandstone lithofacies (fig. 4).

The northwestern boundary of the Emlembe Belt against the Paulus Syncline is a shear zone. Along and adjacent to R40 this zone, included in figure 4 within the Mendon Formation, is a breccia up to 100 m wide composed of blocks of black and banded chert in a sheared matrix of altered komatiitic and mafic volcanic rock. Along the R40 about 1 km from the Eswatini border, the southeastern border of the Emlembe belt shows an Emlembe conglomerate in contact across a well-exposed shear zone about 10 m wide with black chert underlain by volcanic rocks at the top of the Mendon Formation (fig. 3). This black chert is the top of a northwest-facing, overturned section of the upper Onverwacht Group that includes at least members M2c, M2v, M1c, and M1v of the Mendon Formation and K3c, the Footbridge Chert, and underlying volcanic units of the Kromberg Formation (Ferrar & Heubeck, 2018).

The contact of Fig Tree rocks with units of the Mendon Formation is not exposed over most of the Emlembe Belt, but near the R40 at its junction with the Diepgezet Road (figs. 3 and 4), there are two sections in the eastern branch of the Emlembe Belt that show the contact between Emlembe conglomerates and sandstones and underlying rocks of the Onverwacht Group (fig. 4, points B and C). At point C (fig. 4), about 1–2 km north of the R40, there appears to be a conformable east-dipping section that includes altered komatiities of the Mendon Formation overlain by 10–20 m of black and banded Mendon chert, 5–10 meters of silicified fine-grained Fig Tree sandstone and mudstone, and then, at the top, thick quartz-bearing Emlembe sandstone and conglomerate (fig. 9). The basal Fig Tree unit is composed of 5 to 10 meters of fine-grained silicified cross-laminated lithic sandstone and alternating lenses and layers of dark gray, silicified mudstone (fig. 10F). The mudstone units are generally 1–2 cm or less thick and originally formed as thin mud laminations, drapes, and lenses. There is at least one, meter-thick lens of pebble and cobble conglomerate within this section (fig. 9), suggesting that the sandstone-mudstone unit represents a fine-grained facies of the coarser sandstones and conglomerates of the Emlembe sequence. Thick, coarse Emlembe conglomerate with a quartz-bearing sandstone matrix appears 20–40 m above the Mendon chert.

At a second locality, along the R40 about 400 m north of the Diepgezet junction (fig. 4, locality B), volcanic rocks of the Kromberg Formation are overlain with erosional unconformity by quartz-rich Emlembe rocks (fig. 11B). The lowest Emlembe rocks consist of chert-clast conglomerate that mantles and flanks a topographic high of Kromberg volcanic units. The conglomerate is a lenticular unit that ranges from 0 to about 5 m thick and appears to have locally accumulated against a cliff-like face of Kromberg volcanic rocks (fig. 11B). The basal conglomerate, composed largely of rounded to subangular black chert clasts, also contains clasts of underlying Kromberg mafic volcanic rock in the lowest meter and thins and lenses out laterally within 20 m. Similar conglomerate is present a hundred meters to the north along this contact (fig. 11B). The overlying Emlembe conglomerate is composed of a diverse variety of chert clast types and passes laterally to the north into a thick section of mudstone and fine-grained sandstone exposed along the R40 (figs. 4 & 11B).

Sedimentology: The conglomerate that makes up the bulk of the Emlembe Belt is coarse, pebble to cobble, chert-clast, sand-matrix conglomerate. It consists largely of well-rounded chert clasts, has a relatively quartz-rich sandstone matrix, and is largely clast supported. Bedding is poorly defined. The rock is well-sorted overall and lacks muddy material. We infer deposition by aqueous currents, not debris flows. Interbedded and laterally equivalent sandstones locally show well-developed large-scale cross stratification. We have not identified any features suggestive of deposition by surging flows or fine-grained units suggesting intervals of quiet-water sedimentation, as characterize most deep-water sequences. We would suggest that the conglomerates represent a conglomeratic alluvial to fan delta facies

that passes downslope into more distal, sandy, alluvial or shallow-marine facies. The conglomerate that unconformably overlies volcanic and sedimentary rocks of the Kromberg Formation along the R40 (fig. 11B) interfingers to the northeast with Fig Tree mudstones and apparently represents a fringe of shallow-water or terrestrial sediment deposited around the exposed Kromberg units, which may have formed a local hill, and passing laterally within a kilometer into subaqueous muds.

Petrography: Sandstone beds and sandstone matrix to the conglomerates in the Emlembe Belt are composed of three main types of framework grains (fig. 12): (1) coarse monocrystalline quartz (10–50%), (2) chert grains, and (3) lithic grains, represented mainly by microquartz-chlorite or microquartz-sericite aggregates. The coarse quartz occurs as angular to subrounded sand-sized grains, most lacking any clear petrographic indicators of their origin. In a few instances, original grains can be identified by dust coverings and in these cases, the original grains show well-developed irregular syntaxial quartz overgrowths (fig. 12C, D). A few of the original quartz grains show crystal faces and interfacial angles suggesting that it is beta or volcanic quartz, but such grains are rare. Polycrystalline vein and cavity-fill quartz are common. Little or no feldspar was seen in these rocks and there are no voids or other features suggesting that feldspar was originally present.

Chert grains in Emlembe sandstones show a wide variation in the grain size, sorting, and optical properties of the microquartz. Many are carbonaceous chert grains (>5% of the total framework grains) and, among those, there is a high diversity in the types of carbonaceous matter present (fig. 12C, D). Lithic grains are composed mainly of microcrystalline quartz containing fine, irregular chloritic or sericite impurities and irregular particles and masses of opaque matter (fig. 12C, D). Generally, individual samples show only chlorite or sericite in lithic fragments. The chloritic lithic grains, as in the Paulus Syncline, appear to represent silicified mafic to komatiitic debris. It is possible that the chlorite- and sericite-rich rocks are irregularly interstratified or represent distinct facies within this belt. No lithic grains were seen containing feldspars, pseudomorphed feldspars, or quartz phenocrysts.

Shale Geochemistry: Only one mudstone unit was found in the Emlembe Belt that could be sampled for geochemistry (Harrington, 2017; Stoll et al., 2021). The mudstone shows geochemical affinities with more mafic source rocks (fig. 8).

Detrital zircon geochronology: Detrital zircon ages of sandstones from the Emlembe Belt show no evidence of sources younger than about 3.260 Ga and most are dominated by late Mendon-age zircons, ~3.275–3.295 Ga, and by H6 Hooggenoeg-age zircons, ~3.430 to ~3.450 Ga. None of the samples studied (Drabon & Lowe, 2022) shows age peaks <3.260 Ga. We have identified no evidence based on detrital zircons that Emlembe belt sedimentary units are younger than about 3.250–3.260 Ga, although there is a distinct lack of detrital zircons younger than this age throughout the ECD and a corresponding lack of young Fig Tree tuffs or other volcanic units in the stratigraphic section. These detrital zircon results are consistent with derivation of the Emlembe zircons from late Mendon tuffs and H6 felsic volcanic rocks.

Cathodoluminescence studies of Qm: In previous studies of the provenance of quartz and feldspar grains in BGB detrital units we have used cathodoluminescence (CL) studies of quartz and feldspar grains as a helpful indicator of provenance (Lowe & Byerly, 2020). The high Qm contents of sandstones in the Emlembe Belt clearly set them apart from other sandstones in the ECD, and previous investigators including Lowe et al. (2012) have mapped parts of the Emlembe Belt, particularly the western arm, as being composed of Moodies rocks. We have analyzed quartz grains from the Emlembe Belt and associated ECD belts and from potential source rocks, especially older TTG plutons surrounding the BGB and volcaniclastic sandstones of H6 using CL. The CL spectrum of quartz grains in TTG plutonic rocks surrounding the BGB and of quartz grains in volcaniclastic unit H6 in the Hooggenoeg Formation, both potential source rocks for Fig Tree quartz grains, are compared in figure 13A, B. Noteworthy are the very low intensities of the red (640 nm) peak and the broad range of the intensities of the blue (450 nm) peak in quartz from volcanic rocks and the broad range in red peak intensities and low values of blue peak intensities (450 nm) of most plutonic rocks. Only the young (~3.225 Ga) Kaap Valley pluton shows a large spread of blue peak intensities (fig. 13B). Our results from analysis of quartz from sandstones from all ECD belts (fig. 13C, D), including the Emlembe Belt (fig. 13D), suggest that all exhibit low red peak intensities and a broad range of blue peak intensities. These features and the presence of rare beta quartz grain shapes suggests that the elevated quartz contents of Emlembe Belt sandstones as well as of other sandstones in the ECD reflect weathering of quartz-bearing felsic volcanic, not plutonic rocks.

Provenance: The results of this study suggest at least two separate sources contributed debris to sandstones and conglomerates in the Emlembe Belt. The bulk of the debris in conglomerates, sandstones, and shales reflect erosion of older Fig Tree rocks, including jasper and banded ferruginous chert, and Onverwacht sources, notably mafic to komatiitic volcanic rocks and interbedded cherts of the Mendon and possibly Kromberg Formations. Sericite-rich lithic grains and ~3.445 Ga and 3.28–3.295 Ga detrital zircons suggest H6 and uppermost Mendon or lower Fig Tree felsic sources.

A very different source or weathering and transport history is indicated by the high proportion of coarse monocrystalline quartz in Emlembe Belt sandstones, up to a maximum of nearly 50% but overall averaging 25–30%. This abundance contrasts strongly with the <5% Qm in the most Fig Tree sandstones in the Paulus, Manzimnyama, and Mlumati Synclines and suggests either multi-cyclic reworking and quartz-enrichment of the Emlembe sands, more intensive weathering to concentrate first-cycle quartz, a different quartz-rich volcanic source, or some combination of these. However, we emphasize that we have identified no sources of plutonic-derived sediment in the belt or significantly older sedimentary sequences from

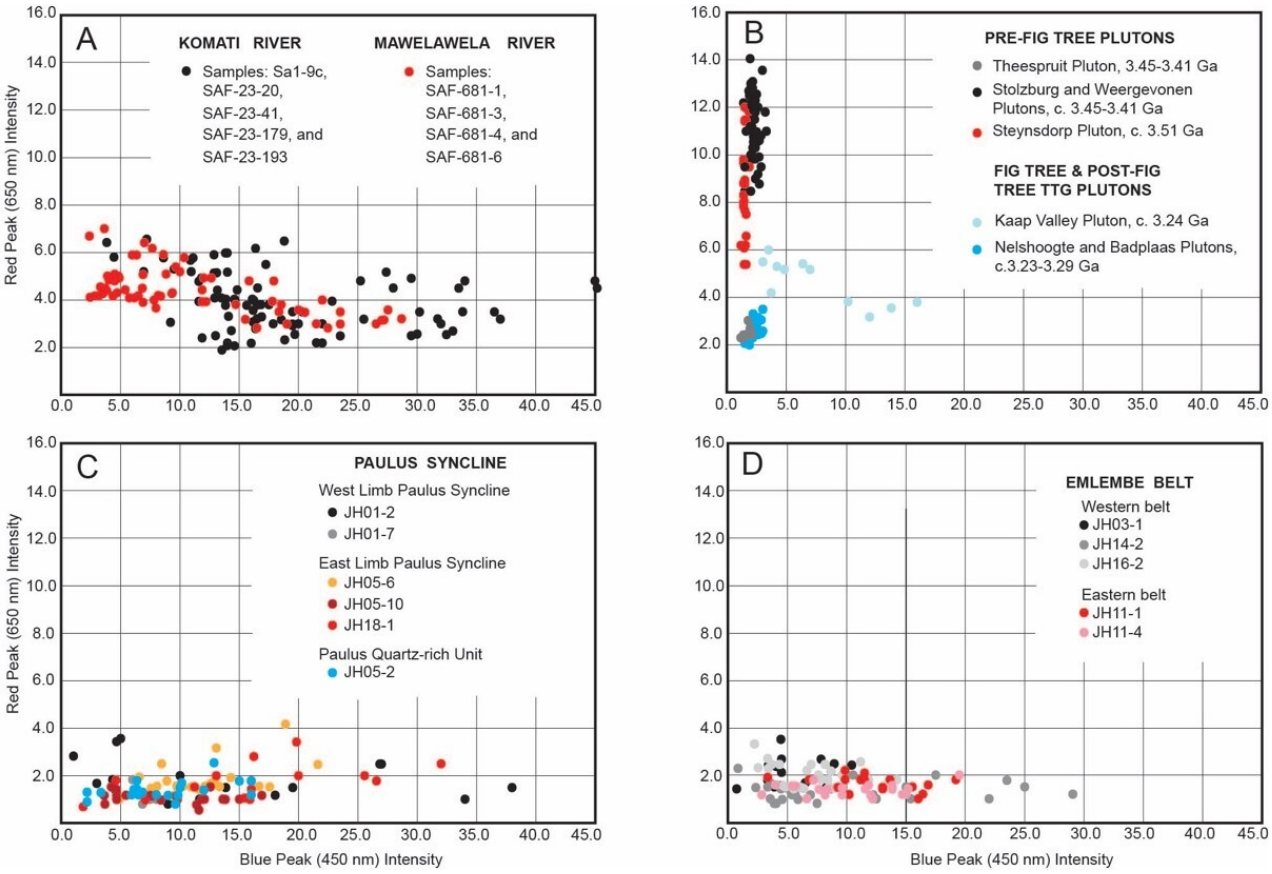

Figure 13. Cathodoluminescence (CL) analysis of quartz grains in the BGB and vicinity. (A, B) From potential igneous source rocks for sediments in the ECD. (A) Quartz from dacitic volcaniclastic rocks of H6 along the Komati River on the east limb of the Onverwacht Anticline and the Mawelawela River on the far west limb of the Onverwacht Anticline (fig. 1). (B) From older and younger generations of plutonic rocks surrounding the Barberton Greenstone belt. (C, D) CL analysis of quartz grains from sandstones in the ECD based on intensities of blue (450 nm) and red (650 nm) peaks. (C) Sandstone samples from the Paulus Syncline. (D) Sandstones from western and eastern arms of the Emlembe Belt. The distributions of red and blue peak intensities are consistent with the grains being of volcanic origin.

which the Emlembe quartz may have been eroded. The apparent absence of plutonic debris is also consistent with the dominance of conglomerate in the Emlembe Belt: most Moodies rocks in the northern BGB, where a plutonic source seems likely, are dominated by sandstone. Coarse granitoid plutonic rocks are the great sand generators of the geologic record. The subordinate amount of sandstone in the Emlembe Belt, the absence of plutonic clasts in the conglomerate, the absence of feldspar, and available CL data all point to non-plutonic, probably felsic volcanic sources for most or all detrital Qm in Emlembe sandstones and conglomerates.

4.2.4. MOODIES GROUP

The problem of distinguishing Fig Tree and Moodies rocks in the eastern BGB has been pointed out by Lamb (1984) and Lamb and Paris (1988). There is no problem when dealing with most Fig Tree rocks in the Manzimnyama, Mlumati, and Paulus Synclines, which have very low Qm (<10% and mostly <5%). However, rocks of the Emlembe Belt have significant quartz contents, with coarse detrital quartz averaging about 20–30% (fig. 7), reaching as high as 50%, with little or no feldspar. Long-recognized Moodies rocks in The Heights Syncline average about 75% Qm (fig. 7) and also largely lack feldspar. Moodies sandstones in The Heights Syncline also contain very little carbonaceous chert (<10%) and that which is present consists mainly of simple, small carbonaceous grains dispersed in a chert matrix (fig. 12E, F). This contrasts with the abundant and complex assemblage of carbonaceous chert grains in Emlembe Belt sandstones (fig. 12C, D). In this study, we have recognized rocks of the Moodies Group only in The Heights Syncline.

5. DISCUSSION

Siliciclastic sedimentary rocks of the Fig Tree Group reflect the first uplift and basin formation in the BGB and one of the earliest known periods of deformation on Earth. From at least 3.55 Ga to about 3.26 Ga, an interval of nearly 300 myr, BGB development was one of predominantly anorogenic mafic to komatiitic volcanism punctuated by episodes of felsic volcanism at ~3.530 Ga (Theespruit Formation) and ~3.445 Ga (H6 member of the Hooggenoeg Formation). In

the BGB, felsic volcanism was accompanied by the development of often steep-sided vents composed of volcanic and volcaniclastic debris and by the erosion of these volcanic centers and dispersal of the debris as surrounding, subaqueous and subaerial aprons of volcaniclastic conglomerate and sandstone (Lowe & Byerly, 2020; M. J. Viljoen & Viljoen, 1969; R. P. Viljoen & Viljoen, 1969).

The Onverwacht sequence that accumulated over this ~300 myr interval appears largely concordant and deposited without major surface deformation and largely without the generation of terrigenous siliciclastic sediment. Shales, terrigenous sandstones, and non-volcanogenic conglomerates are extremely rare in BGB rocks deposited from the deepest exposed levels of the Onverwacht Group to about 3.26 Ga. There are conglomerates and sandstones in member H6 of the Hooggenoeg Formation but these were formed largely due to erosion of the subaerial felsic volcanic edifice and locally of older Onverwacht rocks deformed during magmatic activity (Lowe & Byerly, 2020). Periods of magmatic quiescence throughout accumulation of the Onverwacht Group are marked by mostly thin chert units representing mainly silicified pyroclastic materials, biogenic carbonaceous sediments, and chemical precipitates (Lowe, 1999b). Lowe (2024) has recently suggested that these features of the Onverwacht Group are most consistent with it representing the upper part of a long-lived Paleoarchean stagnant lid.

In this discussion, we will explore the nature of these early, Fig Tree siliciclastic sediments and their implications for the nature of tectonism and for the origins and properties of the basins of deposition in the ECD and elsewhere in the BGB. We would note that the overall thickness, time of formation, and make-up of the BGB sequence are remarkably similar to those of the well-preserved Paleoarchean greenstone sequences in the Pilbara and Singhbhum cratons (Hofmann et al., 2022; Van Kranendonk et al., 2019).

5.1. Detrital zircon dating

Samples from each of the structural belts in the ECD have been analyzed for their detrital zircon ages and very few detrital zircon ages less than about 3.260 Ga have been recorded (Drabon & Lowe, 2022; Harrington, 2017; Stoll et al., 2021; Zentner, 2014). The Gelegela Grit in the Manzimnyama and Mlumati Synclines is dominated almost exclusively by zircons derived from H6-age rocks, 3.445–3.455 Ga. In the Paulus Syncline and Emlembe Belt, detrital rocks are also dominated by H6 zircons and by zircons 3.295–3.275 Ga representing upper Mendon and possibly Loenen sources. There is a notable paucity of post-3.275 Ga zircons and an absence of younger, post-3.26 Ga Fig Tree-age zircons. These relationships are consistent with the paucity of post-Loenen Fig Tree felsic volcanic rocks, ash layers, and tuffaceous sediments in Fig Tree rocks in the ECD and evidently in their source area(s) as well. There are traces of older, pre-3.5 Ga zircons in some samples suggesting sparse exposure of still older units and/or of younger rocks containing older xenocrysts: ~3.500 Ga zircons are common in basal H6 strata along the Komati River (Grosch et al., 2011).

Geochronologically, there is no evidence for deposition of ECD sediments after about 3.26 Ga but stratigraphically there is a suggestion that ECD deposition may have persisted into later Fig Tree time. Rocks in the Southern Domain have been related to those in the ECD by Drabon and Lowe (2022) based on the ~3.277 Ga Loenen- or even slightly older age of the inception of Fig Tree sedimentation in the SD and the presence of a thick Manzimnyama Jaspilite in both areas. The upper part of the SD sequence, above the Manzimnyama Jaspilite, includes the S3 spherule bed (~3.243 Ga) and stratigraphically higher beds containing zircons as young as 3.23 Ga (Drabon & Lowe, 2022). This suggests that the missing upper parts of the ECD sequence could also have included still younger Fig Tree sediments that have not been preserved.

One key Fig Tree ECD date is the 3.260±0.005 Ga SHRIMP age reported here from a thin tuff in the lower Manzimnyama Jaspilite on the east limb of the Manzimnyama Syncline. This age suggests that the overlying Gelegela Grit was deposited after ~3.260 Ga indicating that the initial deposition of the Gelegela Grit roughly coincided with the S2 impact and suggesting that many of the coarse conglomeratic and sandy members at the tops of the ECD Fig Tree sections could also post-date ~3.260 Ga.

5.2. Emlembe Belt: Fig Tree or Moodies?

The Emlembe Belt offers a particular challenge in terms of correlation and tectonic implications both because of its transitional composition between Moodies and Fig Tree rocks elsewhere in the BGB and because of a paucity of age data. The dominance of coarse siliciclastic units in the Emlembe Belt resembles the Moodies Group of more northern areas, such as the Saddleback Syncline (Heubeck, 2019; Heubeck & Lowe, 1999). The Moodies in these areas is composed largely of sandstone with subordinate conglomerate and very little mudrock. However, in detail, Emlembe sedimentary rocks are quite unlike those of either Moodies or Fig Tree units to the north. (1) The Qm composition of Emlembe sandstones is intermediate between Fig Tree and Moodies sandstones, which tend to have <10% Qm or >50% Qm, respectively. The Emlembe Belt sandstones average 20–30% Qm (fig. 7). (2) The Emlembe Belt is composed largely of chert-clast conglomerate with subequal to subordinate sandstone whereas coarse siliciclastic units in both Moodies and Fig Tree Groups to the north are composed largely of sandstone with greatly subordinate conglomerate and have been interpreted to have originated in large part by the erosion of plutonic rocks (Hessler & Lowe, 2006; Heubeck & Lowe, 1999). We would suggest that the reduced amount of sandstone in the Emlembe Belt is due to the lack of plutonic sources of sand-sized sediment, reflected in both the QFL and CL compositions. The Emlembe Belt appears to have been sourced through deep weathering of quartz-bearing volcanic rocks, not plutonic rocks. (3) Emlembe sandstones show much less mature compositions in terms of carbonaceous chert clast abundances and types than Moodies rocks, including those in The Heights Syncline (fig. 11). (4) Also, the Emlembe Belt is unique in the BGB in showing coarse siliciclastic strata lying with ap-

parent conformity on black cherts at the top of the Mendon Formation (locality B, fig. 4). (5) At locality C (fig. 4), coarse Emlembe conglomerate passes laterally into finer sandstone and mudstone resembling those in the Fig Tree Group. These features suggest that the flood of coarse debris began in the Emlembe Belt and perhaps areas farther east very shortly after the close of Onverwacht sedimentation and may have continued concurrently with deposition of finer grained and low-Q Fig Tree strata elsewhere. Unfortunately, the precise age of the initiation of Fig Tree sedimentation in the Emlembe Belt remains uncertain.

5.3. Fig Tree stratigraphic evolution

The Fig Tree Group in the Mlumati, Manzimnyama, and Paulus Synclines shows an overall similar stratigraphic evolution. The base of the sequence is marked by the ~3.277 Ga felsic tuff and volcaniclastic strata of the Loenen member. This water-worked tuffaceous unit has not been seen on the south limb of the Paulus Syncline or in the Emlembe Belt. The Loenen member thickens progressively to the north, consisting of about 5 m of white-weathering tuff in the Mlumati Syncline. This thickness trend suggests an origin of the volcaniclastic debris to the north or northwest.

Upward in the Manzimnyama and Mlumati Synclines, banded ferruginous chert and iron formation predominate with sparse interlayered shales. These fine-grained, laminated cherty sections lack evidence of current or wave activity and reflect sedimentation of fine, largely precipitative sediments under quiet and relatively deep-water conditions (Stoll, 2020; Stoll et al., 2021). The sections are locally punctuated by debris-flow deposits composed of intraformational debris. In the Paulus Syncline, corresponding rocks include thinly banded ferruginous chert and some BIF in the lower 50–100 m of the Fig Tree overlain by several hundred meters of shale and mudstone.

These lower shale- and BIF/BFC-dominated sections pass upward into sections containing lenses and layers of coarse siliciclastic debris. In the Manzimnyama and Mlumati Synclines this upper siliciclastic unit is the Gelegela Grit, a unit of lithic sandstone locally up to 350 meters thick deposited by turbidity currents (Heinrichs, 1980; Stoll et al., 2021; Zentner, 2014). In the Paulus Syncline, the primary coarse units are lenses of chert-clast conglomerate with greatly subordinate, largely quartz-poor (<10% Qm) sandstone. Lenticular chert-clast conglomerate in the middle to upper part of the Paulus Syncline sequence appears to represent channels within which coarse debris was funneled through the system from at least two different sources. The 30-m-thick quartzose sandstone, which overlies a possible alluvial channel, may mark a short-lived, energetic coastal system while the stratigraphically higher chamosite-bearing sediments show evidence for deposition under locally current- and/or wave-active conditions on what appears to be a shallow shelf. The conglomerate in the upper part of the section lacks clear evidence of turbidity current or sediment-flow deposition and probably represents deposition on or in front of small fan deltas. The upper parts of the Fig Tree section in the Mlumati, Manzimnyama, and Paulus Synclines show the coarse clastic layers succeeded by shale or chemical sediments that are the highest units exposed.

Sedimentary units in the Emlembe Belt are coarse throughout except locally where 10–20 m of finer grained silicified sandstone are present at the base overlying black cherts of the Onverwacht Group. Emlembe conglomerates and sandstones have not been analyzed in detail, but the coarse grain size, lack of interbedded mudstone, and presence of large-scale cross-stratification suggest shallow-water, fan delta, and/or subaerial sedimentation. There are no features suggestive of turbidites or deep-water sediments.

In summary, all of the Fig Tree sections in the Mlumati, Manzimnyama, and Paulus Synclines coarsen upward with lower halves dominated by fine-grained siliciclastic and/or chemical sediments succeeded by upper parts showing deposition of coarser material under more energetic and, in some cases, shallow-water to perhaps even subaerial conditions. The final preserved stage of deposition often records a return to deeper water and reduced coarse siliciclastic input. The Emlembe Belt appears to represent shallow-water to fan delta deposits throughout.

The Fig Tree section in Eastern Barite Valley (EBV) in the WCD studied by Drabon, Heubeck et al. (2019) is a well-documented example of this type of Fig Tree evolution (fig. 5B), although this section entirely post-dates the ~3.258 Ga S2 impact while the ECD sections appear to largely predate S2. The EBV section totals about 500–600 m thick. The lower part consists of 150–175 m of shale and mudstone with a few thin sandstone beds. It is marked by S2 (3,258±0.003 Ga; Byerly et al., 1996) at the base and S3 (3,243±0.004 Ga; Kröner et al., 1991) near the top. The overlying coarser-grained units, deposited between about 3.243 and 3.239 Ga and totaling about 175 m thick, shoal upward and reflect sedimentation under shelfal, shallow-marine, and intertidal conditions (Drabon, Heubeck, et al., 2019; Lowe et al., 2019). The uppermost 100+ m of sediment are mainly fine-grained mudstones and tuffaceous sediments with some turbiditic sandstone that appear to range from 3.235 Ga (Drabon, Heubeck, et al., 2019) to perhaps as young as 3.227 Ga (Byerly et al., 1996). Deposition of the basal 175 m of mudstone occurred over an interval of 8 to 22 million years while the overlying coarser, shallow-water sediments, about 150 m thick and representing an influx of materials across prograding fan deltas, occurred over an interval of only about 4 to 10 myr (3.243±0.004 to 3.239±0.001 Ga) following the S3 impact.

5.4. Fig Tree “basin”

One key issue concerns the nature of the “basin” or basins in which Fig Tree Group sediments were deposited (Drabon et al., 2017; Drabon, Galić, et al., 2019; Drabon, Heubeck, et al., 2019; Drabon & Lowe, 2022). Stoll et al. (2021) discussed whether the Emlembe-Paulus-Manzimnyama-Mlumati belts of the ECD represent parts of an originally contiguous transport fairway or source-to-sink deposystem. The coarse fan-delta conglomerates and sandstones of the Emlembe Belt would represent the most proximal parts of the system passing downslope into nearshore coastal deposits and slope channels in the Paulus Syncline to deep-

water basinal deposits of the Manzimnyama and Mlumati Synclines. The time of initiation of Fig Tree sedimentation in these belts appears to be marked by 3.277 Ga Loenen volcanism, although the actual age of the base of the Fig Tree sequence in the Emlembe Belt has yet to be resolved.

All ECD belts except the Emlembe Belt show felsic sources for shales and tuffs toward the base and upward an overall dominance of mafic to komatiitic sources for terrigenous sediments. We consider it likely that this trend reflects increasing exposure and erosion of komatiitic rocks of the Mendon Formation following the initial pulse of Loenen felsic volcanism. However, the middle to upper part of the Manzimnyama Syncline is dominated by the Gelegela Grit representing an abrupt influx of felsic H6-age detritus. This H6 source is unlike those represented by siliciclastic rocks in the Paulus Syncline and Emlembe Belt and distinctly different from very sparse clastic units lower in the Fig Tree in the Manzimnyama Syncline itself, which are composed largely of detrital chert grains. The Paulus Syncline contains a bimodal association of lenticular Qm-poor, chert-clast conglomerate layers, many derived from rocks of the Fig Tree Group itself, and a unit of Qm-rich medium-grained sandstone. The sparse lithic sandstone that does occur in the Paulus Syncline shows lithic grains derived from mafic to komatiitic sources. There is no evidence for felsic sand sources, perhaps accounting for the dearth of sandstone in this belt. The Emlembe Belt is made up of moderate to high Qm sandstone and chert-clast conglomerate. Comparison of the belts suggests that sandstones in each of the belts could not have been part of a common sediment transport fairway. Our results agree with those of Stoll et al. (2021) that the three main belts in the ECD represent different transport fairways and depositional centers, not a large, dismembered southeast-to-northwest transport and depositional system as implied by the foreland basin models of Lowe (1999a) and, to some extent, Drabon and Lowe (2022), although Drabon and Lowe (2022) do recognize that the sediments had varied sources including local uplifts.

Preserved Fig Tree sedimentary rocks in most parts of the WCD, SD, and ECD total less than 1000 m thick (Drabon & Lowe, 2022; Lowe & Byerly, 1999). Deep-water sections in the ND along the northern part of the BGB reach up to 1600 m or perhaps even 2000 m thick (Condie et al., 1970). The rough time span represented by these strata can be estimated by available ages on marker units, including the Loenen member (~3.277 Ga), S2 (~3.257 Ga), S3 (~3.243 Ga), and S5 and associated felsic tuffs (~3.225 Ga). The section in the ECD appears to have been deposited from about 3.277 to about 3.258 Ga, assuming that the absence of S2 in this area can be attributed to the S2 impact occurring after the uppermost strata were deposited. About 700 m of strata were deposited over about 19 to 25 million years (3.277±0.003 to 3.258±0.003 Ga) for an average sedimentation rate, uncorrected for compaction, between 3 and 4 cm/1000 years. Similar thicknesses and intervals of sedimentation can be estimated for Fig Tree strata and the period of Fig Tree deposition elsewhere in the BGB (see sections and age data of Drabon & Lowe, 2022). Throughout the ND, where Fig Tree water depths were relatively deep and sedimentation dominated by sediment flow processes (Condie et al., 1970), somewhat thicker Fig Tree sections are present and deposition occurred mainly between the age of S3, 3.243±0.004 Ga, which marks the base of the Fig Tree section, and about 3.225 Ga, which marks the age of felsic volcaniclastic rocks of the Belvue Road Formation: 1000 to 2000 m of strata were deposited over about 20 million years for a mean sedimentation rate of 7 to 8 cm/1000 years without corrections for compaction.

We are struck by the overall thinness and low sedimentation rates of preserved Fig Tree rocks throughout the BGB compared to those in most Phanerozoic tectonic basins. Phanerozoic tectonic basins commonly contain sediments reaching thousands of meters thick (Abdullayev, 2020). Lowe (1999a) and Drabon and Lowe (2022) have suggested that the Fig Tree represents a foreland basin formed by flexural loading of the crust by a mountain belt to the southeast. Modern foreland basins, however, best seen in ocean-continent or continent-to-continent collision zones, typically have fill totaling thousands of meters thick (e.g., Abdullayev, 2020; DeCelles & Giles, 1996). However, modern continental basins may be imperfect analogs for the BGB and other early Archean basins because available evidence suggests that older continental crust was not involved in development of the Archean basins (Drabon et al., 2017). The BGB appears to have formed in a more oceanic or at least non-cratonic setting until after 3.1 Ga. However, even in modern oceanic arc settings, flanking forearc and backarc basins typically have sediment thicknesses totaling thousands of meters (e.g., Sitchler et al., 2007).

Within the WCD, SD, and ECD, Fig Tree sections that we have studied typically display rapid lateral facies changes, especially of the coarser grained, conglomerate and sandstone units. Conglomerate units are generally a maximum 300–400 m thick and few can be traced for more than a few kilometers along strike: rapid lateral transitions from sandy members into shaly units over 2–4 km or less are common.

The overall characteristics of the Fig Tree Group throughout the BGB speak to a limited coarse-sediment supply, a limited amount of structural uplift, and a limited amount of basinal subsidence. Fig Tree sections are thin, measured in hundreds not thousands of meters compared to those in most Phanerozoic tectonic basins. Fig Tree sediments, while varied, most often seem to document a single major cycle of uplift, erosion, progradation of coarse sediment aprons surrounding the uplifts, and in many cases a late stage of subsidence. Fig Tree stratigraphic evolution typically spanned ~20–30 myr long time intervals, although the major periods of coarse-sediment deposition almost certainly represent much shorter periods of time. In the EBV (fig. 6B), fine muds totaling about 250 m thick were deposited between S2 (~3.257 Ga) and S3 (~3.243 Ga), an interval of about 14 myr, whereas overlying coarse shallow water and fan delta sediments 300 m thick were deposited roughly from the time of S3 (~3.243 Ga) to about the close of barite sedimentation and felsic volcanism at ~3.239 Ga, and interval of 4–5 myr. The overlying section marking subsidence and a return to quiet, subaqueous deposition saw

the accumulation of about 100 m of mainly fine-grained siliciclastic sediment between ~3.239 Ga and 3.227±0.004 Ga (Kröner et al., 1991), about 12 myr (fig. 6B). Deep-water facies in the ND tend to be more laterally continuous, persisting along the entire northern part of the BGB but in the WCD, SD, and ED, most Fig Tree sections show conglomerate and sandstone facies that are laterally discontinuous with rapid facies changes.

Overall, the thickness, distribution, and facies of coarse Fig Tree sediments in the ECD, WCD, and SD seem to represent relatively small fan deltas filling basins with relatively limited accommodation space and sourced by relatively small uplifts. This is consistent with the apparent disparity of sand sources for the various belts, as in the ECD. There is no evidence for large integrated drainage systems or that Fig Tree erosion reached into metamorphosed greenstone units below H6 (about 3000 m below the base of the Fig Tree in the SD) and no evidence that plutonic rocks, which were widely developed at depth representing the ~3445 Ga and ~3500 Ga TTG suites, were exposed to erosion. The sparse detrital zircons of pre-3.445 Ga age could represent reworked xenocrystic old zircons in younger magmatic suites.

Our conclusion is that Fig Tree deformation before about ~3.225 Ga was limited to the formation of small but widespread uplifts. While Fig Tree sedimentation occurred over fairly long periods of time, ~20–35 myr, relatively little sediment accumulated, and the influx of coarse clastic material was limited to a few units mostly just a few hundred meters thick. There is no clear evidence for a long-lived tectonic system that produced major, long-lived uplifts and mountain belts and corresponding long-lived, deep basins like modern continental margins, rifts, foreland settings, or arc-related basins.

5.5. Role of impacts

The initiation of Fig Tree sedimentation was diachronous across the BGB: about 3.277±0.003 Ga (Drabon, Galić, et al., 2019) in the East Central Domain, 3.258±0.003 Ga (Byerly et al., 1996; Drabon & Lowe, 2022) in most of the West-Central Domain, and ~3.243±0.004 Ga (Drabon & Lowe, 2022; Kröner et al., 1991) in the Northern Domain. In two of these areas, the lowest Fig Tree sedimentary rocks are siliciclastic sediments that immediately overlie meteor impact layers, S2 over most of the WCD and S3 in the northernmost WCD and in the ND. In the ECD, Fig Tree sedimentation started with the deposition of the Loenen felsic volcaniclastic units at about 3.277 Ga: no impact layers have been identified to date in the ECD sequence but also, in the Mlumati, Manzimnyama, and Paulus Synclines of the ECD, these lowest layers are not primarily siliciclastic units but rather BFC and/or BIF deposited largey by precipitation out of the ocean. Siliciclastic sedimentation becomes important in the Manzimnyama Sycline only after about 3.260 with deposition of the Gelegela Grit.

The coincidence of large meteor impacts with the abrupt shift from ~300± million years of anorogenic Onverwacht mafic and ultramafic volcanism and pyroclastic, biogenic, and chemical deposition to Fig Tree uplift, deformation, and siliciclastic sedimentation in most parts of the BGB at two different times 15 million years apart bespeaks the strong possibility of a genetic relationship between impacts and the initiation of siliciclastic sedimentation (A. Glikson & Vickers, 2006; Lowe et al., 2003; Lowe & Byerly, 2018). The crustal perturbations were perhaps manifest as widespread fractures, fault-bounded blocks, and/or folds with sediment eroded from the uplifts infilling the intervening low areas. We here suggest the speculative hypothesis that this crustal instability was triggered by the large meteor impacts recorded at the start of and during deposition of siliciclastic sedimentation of the Fig Tree Group. We have previously shown (Lowe et al., 2003; Lowe & Byerly, 2018) that starting possibly as early as the S6 impact at 3.306±0.016 Ga (Drabon et al., 2017), the Earth was subject to a series of large impacts (fig. 2). Between ~3.306 Ga and ~3.277 Ga, Mendon komatiitic volcanism and sedimentation persisted with little or no change. Starting at about ~3.277 Ga, komatiitic volcanism ceased in the ECD, replaced by an interval of quiet and possibly deep-water, largely chemical BFC, BIF, and carbonaceous chert sedimentation.

Coincident with the S2 impact at ~3.258 Ga, crustal instability and deformation formed widespread but overall small and short-lived uplifts and basins. Erosion of the impact-related uplifts and filling of the associated basins produced relatively thin accumulations of Fig Tree sediment over time intervals of 10–25 myr. There is no clear basis for interpreting this early stage of Fig Tree uplift and subsidence as reflecting the existence of an organized, long-lived surface-active geodynamic system. It seems more consistent with short-lived periods of destabilization of an early Archean crust followed by erosion of the impact-generated uplifts and filling of the surrounding impact-generated basins.

H6-age, ~3.445–3.455 Ga zircons are abundant throughout Fig Tree rocks in the ECD (Drabon et al., 2017; Drabon & Lowe, 2022; Stoll et al., 2021). The implied widespread availability of H6 rocks to weathering and erosion during Fig Tree time is belied by the lack or paucity of felsic debris in shales, sandstones, and conglomerates throughout the Paulus and Emlembe belts. Only in the upper part of the Manzimnyama and Mlumati Synclines does the Gelegela Grit reflect a major source of H6-age felsic rocks. In the Paulus Syncline, sandstones overall are subordinate to conglomerates and shales and the sandstones that are present are dominated by chert grains and debris derived from mafic sources. In the Emlembe Belt sandstones show some chert-sericite grains suggesting felsic sources, but these are generally subordinate to mafic debris. These results suggest that H6-age sources provided common detrital zircons but only locally were significant sources of lithic debris. We infer that, except in the case of the Gelegela Grit, most sources of H6 debris were distant, not local uplifts, that most lithic debris was removed by very aggressive weathering (Lowe et al., 2020), and that H6 detrital zircons were widely distributed, perhaps in part by aeolian processes, as has been argued for detrital zircons in the ~3.312 Ga Green Sandstone Bed in M3c member of the Mendon Formation (Lowe et al., 2021). The paucity of felsic lithic debris except

in the Gelegela Grit further suggests that the source for that unit was not a long-lived tectonic uplift but one or more short-lived, impact-generated uplifts that brought to the surface rocks down to H6. The deposition of over 300 m of Gelegela Grit, sharply overlain and underlain by siliciclastic-poor banded iron formation, suggests a rapidly generated, short-lived, non-recurring uplift, consistent with impact-generated relief. The Gelegela Grit lies immediately above and is locally interbedded with the Lower Jaspilite member of the Manzimnyama Jaspilite dated locally at 3.260±5 Ga suggesting the possibility that the S2 impact was the trigger for uplifts that brought rocks as deep as H6 to the surface that sourced the Gelegela Grit. It is noteworthy that 20–50 meters below the lowest siliciclastic turbidites in the Gelegela Grit in outcrops along the R40 highway (Fig. 3), the Manzimnyama Jaspilite contains a 2.75-m-thick debris-flow deposit. This is the Tsunami Conglomerate stop on the Barberton Geotrail (Ferrar & Heubeck, 2018). This debris-flow unit includes a lower division, 2.5 m thick, of intraformational breccia composed of plates of translucent chert, most of which were soft when incorporated into the debris flow and then deposited. The upper 0.25 m is coarse-grained lithic sandstone. This unit marks a major slope failure at about 3.26 Ga that could have been related to the S2 impact. We have not identified any spherules within this deposit.

We suggest that many of the features of the Fig Tree Group in the BGB overall and the ECD in particular are consistent with large impacts playing a major role on crustal development and sedimentation. The marking of the abrupt change from Onverwacht to Fig Tree sedimentation by impact layers S2 and S3, the limited depth and scale of uplifts of the sources of siliciclastic debris represented by Fig Tree clastic rocks, the thinness of Fig Tree basin sequences, and limited supply of coarse siliciclastic debris are all consistent with an impact-related, non-tectonic driver of sedimentation and basin development. Impact events recorded in the Barberton Belt to date (fig. 2 and Lowe et al., 2003; Lowe & Byerly, 1986, 2018) appear to reflect bolides 20 to 50 or perhaps even to 75 km in diameter (Byerly & Lowe, 1994; A. Y. Glikson, 2001; Johnson & Melosh, 2012; Lowe, 2013; Lowe et al., 1989; Lowe & Byerly, 2018), with 2 of the largest being the S2 impact at ~3.258 Ga and the S3 impact at ~3.243 Ga. Deformation resulting from these large impacts would have spread widely across the crust around the impact sites, generating faults, depressions (basins), and uplifts (sediment sources), perhaps some resembling the multi-ringed basins and uplifts associated with Mare Orientale on the moon. Topography generated by crustal deformation associated with such large impacts would have extended for hundreds to thousands of kilometers from the impact sites (Johnson et al., 2016; Zuber et al., 2016). In more proximal areas, erosion of the impact-generated uplifts and sedimentation within adjacent basins would have been associated with the deposition of coarse siliciclastic debris as fan deltas and marine units. The bulk of the exposed uplifts would have been composed of mafic and komatiitic volcanic rocks and cherty sedimentary units that make up the underlying Onverwacht Group. On a hot young Earth (Knauth & Lowe, 1978, 2003; Lowe et al., 2020) aggressive weathering of these uplifts would have produced coarser siliciclastic debris composed of the most refractory components, mainly chert and silicified rocks, and finer-grained muds produced largely through weathering of the mafic and komatiitic rocks. These are just the types of sediments and inferred sources seen in Fig Tree sedimentary rocks. In more distal locations, siliciclastic debris would have been composed largely of muds, as in the EBV section following the S2 impact. The timing of the influx of coarser debris in the EBV section is less well constrained, but in the Mlumati and Manzimnyama Synclines it appears to have been ~3.260 Ga, which would have coincided at least approximately with the S2 impact. Subsequent tectonic instability and tectonic reorganization of the terrestrial crust may have in part overlapped with later impact events, such as the S5 event at 3.225±3 Ga, and may have been influenced by them.

6. CONCLUSIONS

The ECD, which makes up the eastern part of the Barberton Greenstone Belt in South Africa, includes 4 structural belts: from northwest to southeast, the Mlumati, Manzimnyama, and Paulus Synclines, and the Emlembe Belt. While generally similar in stratigraphic development and age, these belts differ in detail in the composition and provenance of their Fig Tree siliciclastic sediments. The Mlumati and Manzimnyama Synclines include very low Qm (<5%) lithic sandstone, the Gelegela Grit, derived almost entirely from H6-age felsic volcanic rocks, but largely lack conglomerate. Similar H6-dominated sandstones are lacking in the other belts. The Paulus Syncline contains some low-Qm (<10%) sandstones, composed in part of altered mafic volcanic debris, but toward the top shows thick conglomerates composed largely of varieties of chert clasts derived from underlying parts of the Fig Tree and Onverwacht Groups. Toward the middle of the Paulus Syncline section there is a distinctive unit up-to-30-m-thick of quartz-rich (>50% Qm) sandstone. All other rocks in this belt are dominated by shale and chert-clast conglomerate with much less abundant, quartz-poor (Qm < 5%) lithic sandstone. The Emlembe Belt is made up largely of coarse, Qm-bearing (ave. 25–30%) sandstone and sand-matrix conglomerate with little mudstone and no low-Qm lithic sandstone. These relationships and contrasts suggest that the four belts in the ECD do not represent a single contiguous fairway of transport and deposition. Their overall similarities suggest that they represent separate basins or parts of a large basin that underwent similar evolutionary histories but differed in local source terrains and depositional settings. The extreme contrasts in stratigraphy, provenance, and, more regionally, age of Fig Tree strata in the various structural belts in the ECD and eastern WCD suggest that the belts may not be dismembered parts of an originally more contiguous Fig Tree basin but represent largely unrelated or only distantly related terranes assembled in post-Fig Tree time.

The distribution and thinness of siliciclastic units in the Fig Tree Group throughout the BGB suggest that the sources of siliciclastic debris were not major tectonic uplifts

and the basins not major sites of long-term subsidence and sediment accumulation, but more local perturbations of the crust that provided local sources of sediment to adjacent, relatively small sedimentary basins. We suggest that the overall properties of Fig Tree sediments across the BGB are most consistent with transitory crustal disturbances associated with large, late Onverwacht and Fig Tree meteor impacts. Prior to about 3.275–3.280 Ga, the age of the Loenen member of the Fig Tree Group in the ECD, the area of the presently exposed BGB was dominated by mafic to komatiitic volcanism. Felsic volcanism occurred in distant locations, represented by detrital zircons and tuffs in younger Fig Tree rocks. There were no known sediment-yielding tectonic uplifts or deformation. This was the final phase of a period of essentially anorogenic magmatism nearly 300+ myr long represented by the Onverwacht Group.

Fig Tree sedimentation in the ECD was initiated at ~3.277±0.003 Ga (Drabon, Galić, et al., 2019) with deposition of Loenen tuffaceous sediments. The overlying Fig Tree Group in the Mlumati and Manzimnyama Synclines to the base of the Gelegela Grit are composed mainly of chemical sediments, BFC and BIF, with minor amounts of shale. While volcanism ceased locally after deposition of the Loenen member, there were few or no local uplifts that sourced course siliciclastic sediments until the deposition of the Gelegela Grit in the Manzimnyama Syncline and conglomerates and sandstones in the Paulus Syncline and possibly the Emlembe Belt. The age of 3.260±0.005 for the lower Manzimnyama Jaspilite on the east limb of the Manzimnyama Syncline suggests that the flood of H6-dominated debris represented by the Gelegela Grit may have been triggered by uplifts associated with the S2 impact at ~3.258 Ga. In the EBV area in the WCD, Fig Tree sedimentation was initiated with widespread mud deposition following the S2 impact but coarse clastic debris did not begin until immediately after the S3 impact at 3.243±0.004 Ga (Kröner et al., 1991). In the ND, Fig Tree sedimentation was initiated following the S3 impact . The S2 and S3 impacts mark local, abrupt transitions from upper Onverwacht komatiitic volcanism and post-volcanism sedimentation to the deposition of chemical and/or siliciclastic sediments of the Fig Tree Group.

Fig Tree deposition in most belts was marked by initially quiet, subaqueous sedimentation of mud or chemical sediments that transitioned upward into floods of coarser siliciclastic debris, often reflecting shallow-water shelf, shoreline, or terrestrial conditions. We suggest that these pulses of coarse sediment reflect the formation and subsequent erosion of impact-generated topography. As the impact-generated highs were eroded down, the adjacent basins filled, and Fig Tree sedimentation gradually ceased without continued tectonic renewal. Throughout most of the BGB, the late stages of Fig Tree deposition were marked by erosion of this topography and a final return to quiet, subaqueous mud or chemical sedimentation. The sediment sources do not appear to have been tectonic uplifts or basins developed through the imposition of a new, long-lasting tectonic regime but basins and uplifts formed through discrete, short-lived events, which we suggest may have been large bolide impacts. However, these episodes of impacting, basin formation, and basin filling had the cumulative effect of weakening the existing crust and, at some point during late- or post-Fig Tree time, there was regional deformation that caused collapse of the greenstone terrain, shortening, and the formation of a series of tight folds and faults, now represented by the main Fig Tree tectonic belts in the BGB. This episode of deformation appears to represent the first stage of collapse and reorganization of a long-lived early Archean crust.

Acknowledgments

We are grateful to Stanford University and Louisiana State University, which provided funds to support this research; to the Sensitive High Resolution Ion Microprobe–Reverse Geometry (SHRIMP-RG) facility in the Stanford Doerr School of Sustainability at Stanford University for many of the analyses; the Stanford Mineral and Microchemical Analysis Facility for the CL analyses and Dale Burns, who oversees the facility; the National Science Foundation, which funded key parts of the early stages of this research; the NASA Exobiology Program grants NCC-2-721, NAG5-98421, and NNG04GM43G to DRL; the Mpumalanga Tourism and Parks Agency, especially Mr. Johan Eksteen, and Sappi Forests, which allowed us access to private lands; and the many mining geologists and interested Barberton residents who have helped the authors in their studies throughout the years. Christoph Heubeck generously loaned us thin sections of Moodies rocks in The Heights Syncline. We are grateful to the International Continental Scientific Drilling Program (ICPP) for access to cores BARB4 and BARB5, which cored rocks of the Fig Tree Group in the Manzimnyama Syncline and eastern Barite Valley, respectively.

Author Contributions

Both authors conducted field work for this study. Petrographic and stratigraphic studies were completed by Lowe, who also wrote the paper. Byerly conducted the microprobe, new zircon dating, and cathodoluminescence analysis.

Editor: C. Page Chamberlain, Associate Editor: Nadja Drabon

Submitted: November 21, 2023 EST, Accepted: July 16, 2024 EST

This is an open-access article distributed under the terms of the Creative Commons Attribution 4.0 International License (CCBY-NC-ND-4.0). View this license's legal deed at https://creativecommons.org/licenses/by-nc-nd/4.0 and legal code at https://creativecommons.org/licenses/by-nc-nd/4.0/legalcode for more information.

REFERENCES

Abdullayev, N. R. (2020). Analysis of sedimentary thickness, volumes and geographic extent of the world sedimentary basins. *Azerbaijan National Academy of Sciences Transactions, Earth Sciences*, *1*, 28–36. https://doi.org/10.33677/ggianas20200100040

Anhaeusser, C. R. (2001). The anatomy of an extrusive-intrusive Archaean mafic-ultramafic sequence: the Nelshoogte Schist Belt and Stolzburg Layered Ultramafic Complex, Barberton Greenstone Belt, South Africa. *South African Journal of Geology*, *104*(2), 167–204. https://doi.org/10.2113/1040167

Arndt, N. T., Wilson, A., Hofmann, A., Mason, P., Bau, M., Byerly, G., & Chunnett, G. (2012). Peering into the cradle of life: scientific drilling in the Barberton Greenstone Belt. *News and Views: Scientific Drilling*, *13*, 71. https://doi.org/10.5194/sd-13-65-2012

Byerly, G. R. (1999). Komatiites of the Mendon Formation: Late-stage ultramafic volcanism in the Barberton Greenstone Belt. *Evolution of the Barberton Greenstone Belt, South Africa. Geological Society of America Special Paper*, *329*, 189–211. https://doi.org/10.1130/0-8137-2329-9.189

Byerly, G. R., Kröner, A., Lowe, D. R., Todt, W., & Walsh, M. M. (1996). Prolonged magmatism and time constraints for sediment deposition in the early Archean Barberton greenstone belt: evidence from the Upper Onverwacht and Fig Tree groups. *Precambrian Research*, *78*(1–3), 125–138. https://doi.org/10.1016/0301-9268(95)00073-9

Byerly, G. R., & Lowe, D. R. (1994). Spinel from Archean impact spherules. *Geochimica et Cosmochimica Acta*, *58*(16), 3469–3486. https://doi.org/10.1016/0016-7037(94)90099-X

Byerly, G. R., Lowe, D. R., & Heubeck, C. (2018). Geologic evolution of the Barberton Greenstone Belt – a unique record of crustal development, surface processes, and early life 3.55 to 3.20 Ga. In *Earth's Oldest Rocks* (pp. 569–613). https://doi.org/10.1016/b978-0-444-63901-1.00024-1

Byerly, G. R., Lowe, D. R., Wooden, J. L., & Xie, X. (2002). An Archean Impact Layer from the Pilbara and Kaapvaal Cratons. *Science*, *297*(5585), 1325–1327. https://doi.org/10.1126/science.1073934

Condie, K. C., & Hunter, D. R. (1976). Trace element geochemistry of Archean granitic rocks from the Barberton region, South Africa. *Earth and Planetary Science Letters*, *29*(2), 389–400. https://doi.org/10.1016/0012-821x(76)90144-8

Condie, K. C., Macke, J. E., & Reimer, T. O. (1970). Petrology and Geochemistry of Early Precambrian Graywackes from the Fig Tree Group, South Africa. *Geological Society of America Bulletin*, *81*(9), 2759–2776. https://doi.org/10.1130/0016-7606(1970)81[2759:PAGOEP]2.0.CO;2

Dann, J. C. (2000). The 3.5 Ga Komati Formation, Barberton Greenstone Belt, South Africa, Part I: New maps and magmatic architecture. *South African Journal of Geology*, *103*(1), 47–68. https://doi.org/10.2113/103.1.47

de Wit, M. J., Hart, R., Martin, A., & Abbott, P. (1982). Archean abiogenic and probable biogenic structures associated with mineralized hydrothermal vent systems and regional metasomatism, with implications for greenstone belt studies. *Economic Geology*, *77*(8), 1783–1802. https://doi.org/10.2113/gsecongeo.77.8.1783

DeCelles, P. G., & Giles, K. A. (1996). Foreland basin systems. *Basin Research*, *8*(2), 105–123. https://doi.org/10.1046/j.1365-2117.1996.01491.x

Dickinson, W. R. (1970). Interpreting detrital modes of graywacke and arkose. *Journal of Sedimentary Petrology*, *40*(2), 695–707. https://doi.org/10.1306/74d72018-2b21-11d7-8648000102c1865d

Dickinson, W. R. (1985). Interpreting provenance relations from detrital modes of sandstones. In *Provenance of Arenites* (pp. 333–361). https://doi.org/10.1007/978-94-017-2809-6_15

Dickinson, W. R., & Suczek, C. A. (1979). Plate tectonics and sandstone compositions. *American Association of Petroleum Geologists Bulletin*, *63*(12), 2164–2182. https://doi.org/10.1306/2F9188FB-16CE-11D7-8645000102C1865D

Drabon, N. (2018). *Crustal Setting, Provenance and Sedimentation in the Paleoarchean Barberton Greenstone Belt, South Africa* [Unpublished Ph.D. Thesis]. Stanford University.

Drabon, N., Galić, A., Mason, P. R. D., & Lowe, D. R. (2019). Provenance and tectonic implications of the 3.28–3.23 Ga Fig Tree Group, central Barberton greenstone belt, South Africa. *Precambrian Research*, *325*, 1–19. https://doi.org/10.1016/j.precamres.2019.02.010

Drabon, N., Heubeck, C. E., & Lowe, D. R. (2019). Evolution of an Archean fan delta and its implications for the initiation of uplift and deformation in the Barberton greenstone belt, South Africa. *Journal of Sedimentary Research*, *89*(9), 849–874. https://doi.org/10.2110/jsr.2019.46

Drabon, N., & Lowe, D. R. (2022). Progressive accretion recorded in sedimentary rocks of the 3.28–3.23 Ga Fig Tree Group, Barberton Greenstone Belt. *Geological Society of America Bulletin*, *134*(5–6), 1258–1276. https://doi.org/10.1130/B35973.1

Drabon, N., Lowe, D. R., Byerly, G. R., & Harrington, J. A. (2017). Detrital zircon geochronology of sandstones of the 3.6-3.2 Ga Barberton Greenstone Belt: No evidence for older continental crust. *Geology*, *45*(9), 803–806. https://doi.org/10.1130/G39255.1

Duchač, K. C., & Hanor, J. S. (1987). Origin and timing of the metasomatic silicification of an early Archean komatiite sequence, Barberton Mountain Land, South Africa. *Precambrian Research*, *37*(2), 125–146. https://doi.org/10.1016/0301-9268(87)90075-1

Ferrar, T., & Heubeck, C. (2018). *Barberton-Makhonjwa Geotrail, Geosites and Viewpoints* (2nd ed.). Hamilton-Fynch for Barberton Tourism and Business Council.

Gehrels, G. E., Valencia, V., & Ruíz, J. (2008). Enhanced precision, accuracy, efficiency, and spatial resolution of U-Pb ages by laser ablation–multicollector–inductively coupled plasma–mass spectrometry. *Geochemistry, Geophysics, and Geosystems*, *9*, 1–13. https://doi.org/10.1029/2007GC001805

Gehrels, G., & Pecha, M. (2014). Detrital zircon U-Pb geochronology and Hf isotope geochemistry of Paleozoic and Triassic passive margin strata of western North America. *Geosphere*, *10*(1), 49–65. https://doi.org/10.1130/GES00889.1

Glikson, A., & Vickers, J. (2006). The 3.26–3.24 Ga Barberton asteroid impact cluster: Tests of tectonic and magmatic consequences, Pilbara Craton, Western Australia. *Earth and Planetary Science Letters*, *241*(1–2), 11–20. https://doi.org/10.1016/j.epsl.2005.10.022

Glikson, A. Y. (2001). The astronomical connection of terrestrial evolution: crustal effects of post-3.8 Ga mega-impact clusters and evidence for major 3.2±0.1 Ga bombardment of the Earth–Moon system. *Journal of Geodynamics*, *32*(1–2), 205–229. https://doi.org/10.1016/S0264-3707(01)00029-1

Grosch, E. G., Kosler, J., McLoughlin, N., Drost, K., Slama, J., & Pedersen, R. B. (2011). Paleoarchean detrital zircon ages from the earliest tectonic basin in the Barberton Greenstone belt, Kaapvaal craton, South Africa. *Precambrian Research*, *191*(1–2), 85–99. https://doi.org/10.1016/j.precamres.2011.09.003

Hanor, J. S., & Duchač, K. C. (1990). Isovolumetric Silicification of Early Archean Komatiites: Geochemical Mass Balances and Constraints on Origin. *The Journal of Geology*, *98*(6), 863–877. https://doi.org/10.1086/629458

Harrington, J. A. (2017). *Using sedimentology and provenance studies to determine depositional relationships between three structural belts of the Ca. 3.22 Ga Fig Tree Group, Barberton Greenstone Belt, South Africa* [Unpublished MS thesis]. Stanford University.

Heinrichs, T. K. (1980). Lithostratigraphische Untersuchungen in der Fig Tree Gruppe des Barberton Greenstone Belt zwischen Umsoli und Lomati (Sudafrika). *Göttinger Arbeiten zur Geologie und Paläontologie*, *22*, 118.

Hessler, A. M., & Lowe, D. R. (2006). Weathering and sediment generation in the Archean: An integrated study of the evolution of siliciclastic sedimentary rocks of the 3.2 Ga Moodies Group, Barberton Greenstone Belt, South Africa. *Precambrian Research*, *151*(3–4), 185–210. https://doi.org/10.1016/j.precamres.2006.08.008

Hessler, A. M., Lowe, D. R., Jones, R. L., & Bird, D. K. (2004). A lower limit for atmospheric carbon dioxide levels 3.2 billion years ago. *Nature*, *428*, 736–738. https://doi.org/10.1038/nature02471

Heubeck, C. (1993). *Geology of the Archean Moodies Group, Barberton Greenstone Belt, South Africa* [Unpublished Ph.D. thesis]. Stanford University.

Heubeck, C. (2019). The Moodies Group–a high resolution archive of Archaean surface processes and basin-forming mechanisms. In *The Archaean Geology of the Kaapvaal Craton, Southern Africa* (pp. 133–169). https://doi.org/10.1007/978-3-319-78652-0_6

Heubeck, C., Engelhardt, J., Byerly, G. R., Zeh, A., Sell, B., Luber, T., & Lowe, D. R. (2013). Timing of deposition and deformation of the Moodies Group (Barberton Greenstone Belt, South Africa): Very-high-resolution of Archaean surface processes. *Precambrian Research*, *231*, 236–262. https://doi.org/10.1016/j.precamres.2013.03.021

Heubeck, C., & Lowe, D. R. (1999). Sedimentary petrography and provenance of the Archean Moodies Group, Barberton Greenstone Belt. *Geologic Evolution of the Barberton Greenstone Belt, South Africa. Geological Society of America Special Paper*, *329*, 259–286. https://doi.org/10.1130/0-8137-2329-9.259

Hofmann, A., Jodder, J., Xie, H., Bolhar, R., Whitehouse, M., & Elburg, M. (2022). The Archaean geological history of the Singhbhum Craton, India – a proposal for a consistent framework of craton evolution. *Earth-Science Reviews*, *228*. https://doi.org/10.1016/j.earscirev.2022.103994

Huber, M. S., & Byerly, G. R. (2018). Volcanological and petrogenetic characteristics of komatiites of the 3.3 Ga Saw Mill Complex, Weltevreden Formation, Barberton Greenstone Belt, South Africa. *South African Journal of Geology*, *121*(4), 463–486. https://doi.org/10.25131/sajg.121.0031

Ingersoll, R. V., Bullard, T. F., Ford, R. L., Grimm, J. P., Pickle, J. D., & Sares, S. W. (1984). The effect of grain size on detrital modes: a test of the Gazzi-Dickinson point-counting method. *Journal of Sedimentary Research*, *54*(1), 103–116. https://doi.org/10.1306/212F83B9-2B24-11D7-8648000102C1865D

Johnson, B. C., Blair, D. M., Collins, G. S., Melosh, H. J., Freed, A. M., Taylor, G. J., Head, J. W., Wieczorek, M. A., Andrews-Hanna, J. C., Nimmo, F., Keane, J. T., Miljković, K., Soderblom, J. M., & Zuber, M. T. (2016). Formation of the Orientale lunar multiring basin. *Science*, *354*(6311), 441–444. https://doi.org/10.1126/science.aag0518

Johnson, B. C., & Melosh, H. J. (2012). Impact spherules as a record of an ancient heavy bombardment of Earth. *Nature*, *485*(7396), 75–77. https://doi.org/10.1038/nature10982

Knauth, L. P., & Lowe, D. R. (1978). Oxygen isotope geochemistry of cherts from the Onverwacht Group (3.4 billion years), Transvaal, South Africa, with implications for secular variations in the isotopic composition of cherts. *Earth and Planetary Science Letters*, *41*(2), 209–222. https://doi.org/10.1016/0012-821X(78)90011-0

Knauth, L. P., & Lowe, D. R. (2003). High Archean climatic temperature inferred from oxygen isotope geochemistry of cherts in the 3.5 Ga Swaziland Supergroup, South Africa. *Geological Society of America Bulletin*, *115*(5), 566–580. https://doi.org/10.1130/0016-7606(2003)115%3c0566:hactif%3e2.0.co;2

Kröner, A., Byerly, G. R., & Lowe, D. R. (1991). Chronology of early Archaean granite-greenstone evolution in the Barberton Mountain Land, South Africa, based on precise dating by single zircon evaporation. *Earth and Planetary Science Letters*, *103*(1–4), 41–54. https://doi.org/10.1016/0012-821X(91)90148-B

Kröner, A., Hegner, E., Wendt, J. I., & Byerly, G. R. (1996). The oldest part of the Barberton granitoid-greenstone terrain, South Africa: evidence for crust formation between 3.5 and 3.7 Ga. *Precambrian Research*, *78*(1–3), 105–124. https://doi.org/10.1016/0301-9268(95)00072-0

Lamb, S. H. (1984). *Geology of part of the Archaean Barberton Greenstone Belt, Swaziland* [Unpublished Ph.D. dissertation]. Cambridge University.

Lamb, S., & Paris, I. A. (1988). Post-Onverwacht group stratigraphy in the SE part of the Archaean Barberton greenstone belt. *Journal of African Earth Sciences*, *7*, 285–306. https://doi.org/10.1016/0899-5362(88)90074-7

Lowe, D. R. (1982). Sediment gravity flows; II, Depositional models with special reference to the deposits of high-density turbidity currents. *Journal of Sedimentary Research*, *52*(1), 279–297. https://doi.org/10.1306/212F7F31-2B24-11D7-8648000102C1865D

Lowe, D. R. (1999a). Geologic evolution of the Barberton Greenstone Belt and vicinity. *Geological Society of America Special Paper*, *329*, 287–312. https://doi.org/10.1130/0-8137-2329-9.287

Lowe, D. R. (1999b). Petrology and sedimentology of cherts and related silicified sedimentary rocks in the Swaziland Supergroup. *Geological Society of America Special Paper*, *329*, 83–114. https://doi.org/10.1130/0-8137-2329-9.83

Lowe, D. R. (2013). Crustal fracturing and chert dike formation triggered by large meteorite impacts, ca. 3.260 Ga, Barberton greenstone belt, South Africa. *Geological Society of America Bulletin*, *125*(5–6), 894–912. https://doi.org/10.1130/b30782.1

Lowe, D. R. (2024). Onverwacht Group, Barberton Greenstone Belt, South Africa: 300 m.y. development of a Paleoarchean stagnant lid. *Geological Society of America Bulletin*. https://doi.org/10.1130/B37573.1

Lowe, D. R., & Byerly, G. R. (1986). Early Archean silicate spherules of probable impact origin, South Africa and Western Australia. *Geology*, *14*(1), 83–86. https://doi.org/10.1130/0091-7613(1986)14%3c83:EASSOP%3e2.0.CO;2

Lowe, D. R., & Byerly, G. R. (1999). Stratigraphy of the west-central part of the Barberton Greenstone Belt, South Africa. *Geologic Evolution of the Barberton Greenstone Belt, South Africa. Geological Society of America Special Paper*, *329*, 1–36. https://doi.org/10.1130/0-8137-2329-9.1

Lowe, D. R., & Byerly, G. R. (2018). The terrestrial record of Late Heavy Bombardment. *New Astronomy Reviews*, *81*, 39–61. https://doi.org/10.1016/j.newar.2018.03.002

Lowe, D. R., & Byerly, G. R. (2020). The non-glacial and non-cratonic origin of an early Archean felsic volcaniclastic unit, Barberton Greenstone Belt, South Africa. *Precambrian Research*, *341*, 105647. https://doi.org/10.1016/j.precamres.2020.105647

Lowe, D. R., Byerly, G. R., Asaro, F., & Kyte, F. J. (1989). Geological and Geochemical Record of 3400-Million-Year-Old Terrestrial Meteorite Impacts. *Science*, *245*(4921), 959–962. https://doi.org/10.1126/science.245.4921.959

Lowe, D. R., Byerly, G. R., & Heubeck, C. (1999). Structural divisions and development of the west-central part of the Barberton Greenstone Belt. *Geologic Evolution of the Barberton Greenstone Belt, South Africa. Geological Society of America Special Paper*, *329*, 37–82. https://doi.org/10.1130/0-8137-2329-9.37

Lowe, D. R., Byerly, G. R., & Heubeck, C. E. (2012). Geologic map of the West-Central Barberton Greenstone Belt, South Africa. *Geological Society of America Map and Chart Series*, MCS103.

Lowe, D. R., Byerly, G. R., Kyte, F. T., Shukolyukov, A., Asaro, F., & Krull, A. (2003). Spherule beds 3.47-3.24 billion years old in the Barberton Greenstone Belt, South Africa: A record of large meteorite impacts and their influence on early crustal and biological evolution. *Astrobiology*, *3*(1), 7–48. https://doi.org/10.1089/15311070332163240

Lowe, D. R., Byerly, G. R., Ransom, B. L., & Nocita, B. W. (1985). Stratigraphic and sedimentological evidence bearing on structural repetition in early Archean rocks of the Barberton greenstone belt, South Africa. *Precambrian Research*, *27*(1–3), 165–186. https://doi.org/10.1016/0301-9268(85)90011-7

Lowe, D. R., Drabon, N., & Byerly, G. R. (2019). Crustal fracturing, unconformities, and barite deposition, 3.26–3.23 Ga, Barberton Greenstone Belt, South Africa. *Precambrian Research*, *327*, 34–46. https://doi.org/10.1016/j.precamres.2019.02.024

Lowe, D. R., Drabon, N., Byerly, G. R., & Byerly, B. L. (2021). Windblown Hadean zircons derived by erosion of impact-generated 3.3 Ga uplifts, Barberton Greenstone Belt, South Africa. *Precambrian Research*, *356*, 106111. https://doi.org/10.1016/j.precamres.2021.106111

Lowe, D. R., Ibarra, D. E., Drabon, N., & Chamberlain, C. P. (2020). Constraints on surface temperature 3.4 billion years ago based on triple oxygen isotopes of cherts from the Barberton Greenstone Belt, South Africa, and the problem of sample selection. *American Journal of Science*, *320*(9), 790–814. https://doi.org/10.2475/11.2020.02

Lowe, D. R., & Nocita, B. W. (1999). Foreland basin sedimentation in the Mapepe Formation, southern-facies Fig Tree Group. *Geologic Evolution of the Barberton Greenstone Belt, South Africa. Geological Society of America Special Paper*, *329*, 233–258. https://doi.org/10.1130/0-8137-2329-9.233

Paris, I. A. (1984). *The geology of the farms Josefsdal, Dunbar and part of Diepgezet in the Barberton greenstone belt* [Unpublished PhD. Thesis]. University of the Witwatersrand.

Paris, I., Stanistreet, I. G., & Hughes, M. J. (1985). Cherts of the Barberton Greenstone Belt interpreted as products of submarine exhalative activity. *The Journal of Geology*, *93*(2), 111–129. https://doi.org/10.1086/628935

Sitchler, J. C., Fisher, D. M., Gardner, T. W., & Protti, M. (2007). Constraints on inner forearc deformation from balanced cross sections, Fila Costeña thrust belt, Costa Rica. *Tectonics*, *26*(6). https://doi.org/10.1029/2006TC001949

Stiegler, M. T., Cooper, M., Byerly, G. R., & Lowe, D. R. (2012). Geochemistry and petrology of komatiites of the Pioneer Ultramafic Complex of the 3.3 Ga Weltevreden Formation, Barberton greenstone belt, South Africa. *Precambrian Research*, *212–213*, 1–12. https://doi.org/10.1016/j.precamres.2012.04.017

Stoll, E. (2020). *Provenance and sedimentology of the Archean Mapepe Formation, southeastern Barberton Greenstone Belt, South Africa* [Unpublished MS thesis]. Stanford University.

Stoll, E., Drabon, N., & Lowe, D. R. (2021). Provenance and paleogeography of Archean Fig Tree siliciclastic rocks in the East-Central Barberton Greenstone Belt, South Africa. *Precambrian Research*, *354*, 106041. https://doi.org/10.1016/j.precamres.2020.106041

Tice, M. M., Bostick, B. C., & Lowe, D. R. (2004). Thermal history of the 3.5–3.2 Ga Onverwacht and Fig Tree Groups, Barberton greenstone belt, South Africa, inferred by Raman microspectroscopy of carbonaceous materials. *Geology*, *32*(1), 37–40. https://doi.org/10.1130/G19915.1

Tice, M. M., & Lowe, D. R. (2006). The origin of carbonaceous matter in pre-3.0 Ga greenstone terrains: A review and new evidence from the 3.42 Ga Buck Reef Chert. *Earth-Science Reviews*, *76*, 259–300. https://doi.org/10.1016/j.earscirev.2006.03.003

Van Kranendonk, M. J., Kröner, A., Hegner, E., & Connelly, J. (2009). Age, lithology and structural evolution of the c. 3.53 Ga Theespruit Formation in the Tjakastad area, southwestern Barberton Greenstone Belt, South Africa, with implications for Archaean tectonics. *Chemical Geology*, *261*(1–2), 115–139. https://doi.org/10.1016/j.chemgeo.2008.11.006

Van Kranendonk, M. J., Smithies, R. H., & Champion, D. C. (2019). Paleoarchean development of a continental nucleus: The East Pilbara Terrane of the Pilbara Craton, Western Australia. In *Earth's Oldest Rocks* (2nd ed., pp. 437–462). https://doi.org/10.1016/B978-0-444-63901-1.00019-8

Viljoen, M. J., & Viljoen, R. P. (1969). The geology and geochemistry of the lower ultramafic unit of the Onverwacht Group and a proposed new class of igneous rocks. *Geological Society of South Africa, Special Publication 2*, 55–86.

Viljoen, R. P., & Viljoen, M. J. (1969). The geological and geochemical significance of the upper formations of the Onverwacht Group. *Geological Society of South Africa, Special Publication 2*, 113–152.

Walsh, M. M. (1989). *Carbonaceous Cherts of the Swaziland Supergroup, Barberton Mountain Land, Southern Africa* [PhD thesis, Louisiana State University]. https://doi.org/10.31390/gradschool_disstheses.4751

Walsh, M. M., & Lowe, D. R. (1999). Modes of accumulation of carbonaceous matter in the early Archean: A petrographic and geochemical study of the carbonaceous cherts of the Swaziland Supergroup. *Geologic Evolution of the Barberton Greenstone Belt, South Africa. Geological Society of America Special Paper*, *329*, 115–132. https://doi.org/10.1130/0-8137-2329-9.115

Xie, X., Byerly, G. R., & Ferrell, R. E., Jr. (1997). IIb trioctahedral chlorite from the Barberton greenstone belt: crystal structure and rock composition constraints with implications to geothermometry. *Contributions to Mineralogy and Petrology*, *126*(3), 275–291. https://doi.org/10.1007/s004100050250

Zentner, D. B. (2014). *Stratigraphy, sedimentology and provenance of the ca. 3.26 Ga Mapepe Formation in the Manzimnyama Syncline, Barberton Greenstone Belt, South Africa* [Unpublished MS Thesis]. Stanford University.

Zuber, M. T., Smith, D. E., Neumann, G. A., Goossens, S., Andrews-Hanna, J. C., Head, J. W., Kiefer, W. S., Asmar, S. W., Konopliv, A. S., Lemoine, F. G., Matsuyama, I., Melosh, H. J., McGovern, P. J., Nimmo, F., Phillips, R. J., Solomon, S. C., Taylor, G. J., Watkins, M. M., Wieczorek, M. A., ... Yuan, D.-N. (2016). Gravity field of the Orientale basin from the gravity recovery and interior laboratory mission. *Science*, *354*(6311), 438–441. https://doi.org/10.1126/science.aag0519